

ALP production in weak mesonic decays

A.W.M. GUERRERA^a AND S. RIGOLIN^{a,b}

^a *Istituto Nazionale Fisica Nucleare, Sezione di Padova*

^b *Dipartimento di Fisica e Astronomia “G. Galilei”,
Università degli Studi di Padova, I-35131 Padova, Italy*

Abstract

Axion-Like-Particles are among the most economical and well motivated extensions of the Standard Model. In this work ALP production from hadronic and leptonic meson decays are studied. The hadronization part of these decay amplitudes have been obtained using Brodsky-Lepage method or LQCD, at needs. In particular, the general expressions for ALP emission in mesonic s- and t-channel tree-level processes are thoroughly discussed, for pseudoscalar and vector mesons. Accordingly, the calculation of the decay amplitudes for $M_I \rightarrow M_F a$ and $M \rightarrow \ell \nu a$ are presented. Finally, bounds on the (low-energy effective Lagrangian) ALP-fermion couplings are derived, from present and future flavor experiments.

1 Introduction

Light pseudoscalar particles are a common feature of many extensions of the Standard Model (SM) of particle physics. These can be naturally introduced in beyond SM (BSM) scenarios, following the QCD axion paradigm [1–4], as pseudo Nambu-Goldstone bosons (pGBs) of a global $U(1)_{PQ}$ symmetry, non-linearly realized, spontaneously broken at a scale $f_a \gg v$, where v is the Higgs VEV. The main difference between the QCD axion and an Axion Like Particle (ALP) lies in abandoning the requirement that the only explicit breaking of the $U(1)_{PQ}$ symmetry arises from non-perturbative QCD effects [4], imposing the well known relation $m_a f_a \approx m_\pi f_\pi$. Therefore, allowing the ALP mass m_a and the PQ symmetry breaking scale f_a to be independent parameters gives rise to an abundance of scenarios populated by scalar singlets under the SM group, not necessarily tied to the solution of the Strong CP problem [5–9]. Notable BSM theories that include light singlet scalar fields are: string theory models [10], familons [11,12], flaxions [13,14] and relaxions [15]. ALPs, regardless the naturalness problem they are called to solve, represent compelling candidates for explaining DM abundance in our Universe [16–18]. Whatever is the scenario considered, due to the pGB origin of the ALP, it may be plausible that the first hints of New Physics (NP) at the f_a scale could be hidden in low-energy observables.

The most general CP conserving effective Lagrangian, including operators up to dimension five [19], and describing ALP interactions with SM fermions and gauge bosons, is given by:

$$\delta\mathcal{L}^a = -\frac{\partial_\mu a}{2f_a} \bar{f} \gamma^\mu (C_V + C_A \gamma^5) f - \frac{\partial_\mu a}{f_a} \sum_X c_X X_{\mu\nu}^a \tilde{X}^{\mu\nu a}, \quad (1)$$

where C_V and C_A are hermitian matrices in flavor space, a is the ALP field, f are the SM fermions and $X_{\mu\nu}^a$ indicates any SM gauge boson field strength, with $\tilde{X}^{\mu\nu a} \equiv X_{\alpha\beta}^a \epsilon^{\alpha\beta\mu\nu}/2$. Note that the flavor conserving diagonal vector couplings are identically zero up to a shift in the electroweak anomalous coupling. Following most of the literature [20–25], a low-energy CP and flavor conserving effective Lagrangian for ALP-fermion interactions can be introduced:

$$\delta\mathcal{L}_{\text{ferm}}^a = -\frac{\partial_\mu a}{2f_a} c_i \bar{f}_i \gamma^\mu \gamma^5 f_i = i \frac{a}{f_a} m_i \bar{f}_i \gamma^5 c_i f_i. \quad (2)$$

The index i extends over all the fermions but the neutrinos, assumed to be massless, with c_i real, but not universal, ALP-fermions couplings. With the Lagrangian of Eq. (2) all flavor-violating effects will be loop induced and CKM suppressed,¹ in the spirit of the Minimal Flavor Violation (MFV) ansatz [27].

¹In more general frameworks flavor violating couplings can be introduced at tree level [12,23,26], and limits on these parameters can be simply recovered by removing the loop factors and the CKM suppression.

Most of the attention in the past has been devoted in constraining ALPs couplings with gauge bosons, mainly photons and gluons. In particular, very stringent bounds on c_γ can be obtained from astrophysical searches: helioscopes [28–31], haloscopes [32–35], anomalies in stellar evolution [36, 37] or helioseismology [38]. ALP-fermions couplings can be studied in astro-particles/DM experiments like XENON [39, 40] or CASPER [41] and ARIADNE [42] or using astrophysical data, like for example supernova γ -ray emission [43]. All these searches are, however, limited to very light ALP masses, rarely heavier than few hundreds of eV, and, moreover, they can only bound first generation ALP-fermion couplings. Therefore, terrestrial beam experiments are complementary in the exploration of the ALP couplings parameter space, and, among them, flavor factories are very likely the most promising ones.

Flavor physics experiments have received more and more attention from the phenomenological community [21, 23–25, 44, 45]. Strong limits on the ALP couplings in Eq. (1) can be derived, for example, through the study of the $K \rightarrow \pi a$ decay. In large part of the literature a flavor universal ALP-fermion coupling, often dubbed $c_{a\Phi}$, is assumed. In this scenario, the $K \rightarrow \pi a$ amplitude is penguin dominated² and one can bound c_W and $c_{a\Phi}$ at the level of 10^{-3} for $f_a = 1$ TeV [21]. However, several models have been introduced where large hierarchies between axion couplings [46–49] are naturally produced. It is then of foremost phenomenological relevance to scan the ALP couplings parameter space following a less unbiased approach and to identify case by case which limits can be extracted from a given experiment on each independent ALP-fermion coupling. For example, in a non-universal ALP-fermion coupling scenario, the strongest limit from the $K \rightarrow \pi a$ decay is obviously obtained for the ALP-top coupling, $c_t \approx c_{a\Phi} \lesssim 10^{-3}$ for $f_a = 1$ TeV, due to the penguin top-mass enhancing. However, being the charm penguin contribution to the $K \rightarrow \pi a$ roughly 10% of the top one, an independent bound on the ALP-charm coupling, $c_c \lesssim 10^{-2}$, can be derived, assuming all the other ALP couplings vanishing. Moreover, as noticed by [24], the $K \rightarrow \pi a$ decays can also be mediated by tree-level diagrams with a W^\pm -boson exchanged in the s-channel (t-channel) for charged (neutral) K decays. These diagrams contribute at the 1% level to the total decay amplitude and therefore one can extract independent limits on the ALP-lighter quark couplings, $c_{u,d,s} \lesssim 10^{-1}$ for $f_a = 1$ TeV, for most of the kinematically allowed m_a range.

However, one of the main obstacles in calculating hadronic observables is to deal with the associated non-perturbative matrix element. In treating transitions mediated by local operators, like for example penguin contributions with heavy virtual particles in the loop, one can make use of the available Lattice QCD results [50]. Conversely, to compute products of bi-local operators mediated by virtual light states,

²It has to be recalled that this strong bound mainly arises from the top-penguin diagrams, due to the large top-mass enhancement.

alternative methods, like for example the Brodsky–Lepage technique [51–53], have to be used [24]. Only when the calculation of all these different contributions is done explicitly, one can fairly compare the sensitivity reach on ALP-fermion couplings of the different mesonic decay channels.

From the previous discussion one realizes immediately that, differently from what naively expected, present experiments can already provide a full set of constraints on the possible ALP–fermion flavor structures, therefore motivating a thorough study of mesonic ALPs rare decays. In this work two wide classes of mesonic decays in ALP are considered: *i*) the mesonic decays $M_I \rightarrow M_F a$, with M_I and M_F being either a pseudoscalar or a vector meson and *ii*) the leptonic meson decay processes, $M \rightarrow \ell \nu a$. In all these processes an “invisible” ALP is assumed, i.e. the ALP lifetime is sufficiently long for escaping the detector (typically $\tau_a \geq 100$ ps) or alternatively the ALP is mainly decaying in a, not better specified, invisible sector.

The flagship process for ALP searches in flavor transitions is undoubtedly the $K \rightarrow \pi + \cancel{e}$ signature, studied at NA62 [54–57] and KOTO [58], that arises from a $s \rightarrow d a$ transition at the quark level. Kaon physics is thus in the spotlight for probing ALP couplings in the KeV to hundreds of MeV ALP-mass region. B -factories have also a fundamental impact in limiting the ALP–fermion coupling parameter space. BaBar, Belle [59–66] and LHCb [67, 68] are carefully analyzing visible and invisible signatures of b -meson decays. For example, Belle experiment had conducted searches for $B \rightarrow M_F \bar{\nu} \nu$ for many different mesonic final states M_F , testing ALP masses up to a few GeV. Conversely, measurements of D mesons decays with final state composed of a meson and missing energy are missing at the moment [69]. Another class of interesting processes for probing ALP–fermion physics is represented by decays with a mono- $\gamma + \cancel{e}$ signature. Flavor conserving Υ resonant searches exploiting decays such as $\Upsilon(nS) \rightarrow \Upsilon(1S) \pi^+ \pi^-$ can be used to directly probe $\Upsilon(1S) \rightarrow \gamma + \cancel{e}$ decays [70].

The paper is organized as follows: in Sec. 2 a general discussion on the hadronization techniques needed for calculating pseudoscalar and vector meson decays in ALP is presented. In Sec. 3 the mesonic decay amplitudes in ALPs needed for calculating hadronic and leptonic meson decays in ALP are derived in general. Many of these amplitudes have been calculated here for the first time. Useful phenomenological approximation are discussed for each channel. Section 4 is devoted to describe the phenomenological impact of ALP emission in weak-induced meson decays, assuming an invisible ALP in the final state. All the relevant charged and neutral meson hadronic decays in ALP are estimated at tree and/or at one-loop (penguin) level. Derived bounds on ALP–fermion couplings from hadronic and leptonic meson decays are then discussed and a complete summary of the present situation is shown. Finally, for completeness, in Appendix A exclusion bounds on flavor changing ALP-fermion parameters are presented, for two different scenarios.

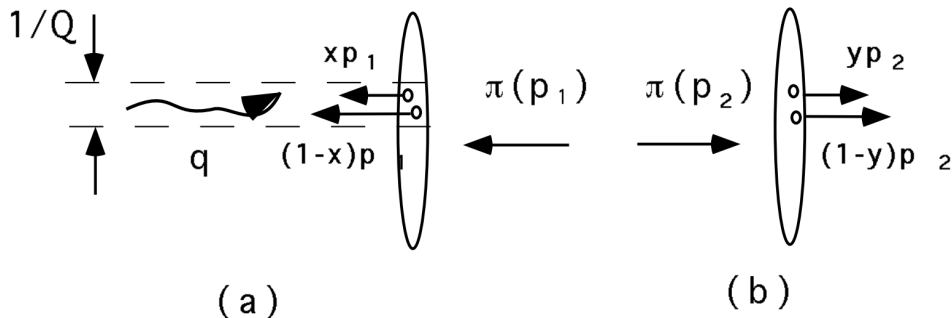


Figure 1: The valence quark state of a pion interacting with an external current carrying momentum Q . The valence couple must be localized in $1/Q$ in the transverse direction while in the longitudinal one Lorentz contraction assures the partons to be close. The picture is taken from [72].

2 Mesonic Hadronization

Despite the fact that in their rest frame mesons and baryons are complex non-static objects, they interact with highly relativistic particles mostly through their valence quark content, justifying a simplified description of these non-perturbative states [51–53, 71, 72]. In the case at hand, the relevant observation is that the final state particles, when recoiling back to back must be emitted in a highly relativistic state. Therefore, the strong quantum effects that bind the meson constituents appear highly time-dilated, and the partonic content looks frozen, to the light escaping particle. For relative speeds near the speed of light the two recoiling particles are in contact for a very short time, decreasing as $(1 - v^2/c^2)^{1/2}$. The relevant interactions can then only happen on small time scales and distances, relatively to typical mesonic masses and sizes, where QCD is perturbative. As such, the short-distance and the long-distance dynamics will have practically no interference. This incoherence between soft and hard physics implies that each meson, during the entire interaction with a highly relativistic particle, can be approximated with its partonic structure allowing for a significant simplification. The long-time dynamic of the initial state is described by the valence quarks Distribution Amplitude (DA) function, $\phi_I(x)$, representing the probability of finding the valence quarks of the incoming meson with a certain meson momentum fraction x . On the other side, the short-distance interaction between the meson quarks and the ALP is described by the hard-scattering amplitude $\Gamma(x, y, Q, \mu)$. Eventually, at a later time, quarks reform the outgoing meson, again described via a DA function, $\phi_F(x)$. The total amplitude for the process

at hand can then be written as a convolution of the three probabilities:

$$\langle M_F | \Gamma | M_I \rangle = \int dx dy \left(\phi_F^*(y, \mu) \otimes \Gamma(x, y, \mathcal{Q}, \mu) \otimes \phi_I(x, \mu) \right) \left(1 + \mathcal{O}(m_q^2/\mathcal{Q}^2) \right) \quad (3)$$

where m_q is the mass of the lightest quark of the meson and $\Gamma(x, y, \mathcal{Q}, \mu)$ is to be expanded perturbatively. In Eq. (3) \mathcal{Q} is the exchanged momentum, x, y indicate the fraction of momentum carried by the heaviest parton of the initial and final meson respectively and μ is the renormalization scale. A natural choice is $\mathcal{Q} = \mu$, making the perturbative calculation consistent as long as $\alpha_s(\mathcal{Q})$ is perturbative. The length associated to this momentum exchange, $b = 1/\mathcal{Q}$, represents the localization of the valence quarks in the transverse plane, relative to the mesons motion as pictorially shown in Fig. 1. If partons are separated more than b that particular state will not contribute to the amplitude. Three particle states, e.g. with an extra gluon, will be suppressed by extra $1/\mathcal{Q}$ factors, since the probability of finding more than the minimum number of particles bunched up in $1/\mathcal{Q}$ decreases as \mathcal{Q} grows. For a simple hard gluon exchange between two fermionic currents the classical dimension of the hard scattering amplitude is $(\text{mass})^{-2}$ and since the dependence has to come from external momenta the approximate form of the hard amplitude can be expressed as

$$\frac{1}{(xy \mathcal{Q}^2)} + \frac{1}{((1-x)(1-y) \mathcal{Q}^2)}.$$

The end-point values, $x, y \simeq 0, 1$, can be problematic as they violate the localization assumption and generate unphysical singularities. Indeed, for these values the hard scattering function spreads out in transverse space and it will not be anymore concentrated around the $1/\mathcal{Q}$ region. The physical picture corresponds to the case of a fast parton–slow parton couple. The slow parton will have $E \approx \Lambda_{QCD}$ and its superposition with more complicated external states is not evidently suppressed and indicates a failure of the localization assumption. A very asymmetric, somewhat long-range configuration has to be superimposed with the soft external states to estimate the contribution at the end-points. It can be shown, however, that in the large momentum exchange limit [51, 73–75] these contributions are typically suppressed by extra factors of m_q/\mathcal{Q} and can be safely neglected as a first order approximation.

2.1 Distribution Amplitudes

The simplest way to implement the factorization mechanism described in the previous section is via the theory of QCD exclusive processes, firstly developed by Brodsky and Lepage [51, 52]. The calculation has two main ingredients, the momentum DA, ϕ_i , introduced in Eq. (3) and the hard scattering amplitude. Indeed, the localization

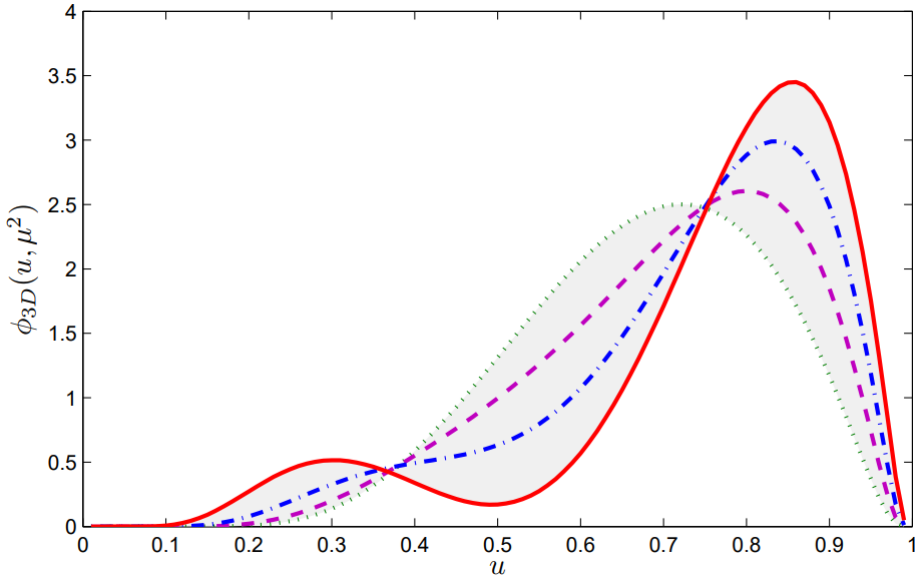


Figure 2: The D meson distribution amplitude ϕ_D at $\mu = 1$ GeV (from [76]). The dotted, the dashed, the dash-dot and the solid lines are for different values of the Gegenbauer momentum $B_D = 0, 0.20, 0.40$ and 0.60 respectively.

assumption and the relativistic view discussed at the beginning of Sec. 2 can be used to build the probability distributions of the valence quarks in momentum space, thus recovering their DAs [51, 52, 76–79].

Let's consider for the moment the case of a light meson M_L of total momentum P_M and let's label with (\mathbf{p}_T, xP_M) , the three-momenta of one of its partons. The 2-component vector $\mathbf{p}_T = (p_x, p_y)$ spans the plane transverse to the direction of motion of the meson, while x is the fraction of the meson momentum carried by the considered parton. Imposing the bound-state valence quarks approximation (i.e. localization) amounts to taking the part of the probability distribution dependent on its transverse momentum as an harmonic oscillator solution, namely:

$$\psi_L(x, \mathbf{p}_T) = A_L G_L(x) \exp\left(-\frac{\mathbf{p}_T^2 + m_q^2}{8\beta_L^2(1-x)x}\right), \quad (4)$$

where A_L is an normalization constant and β_L is a mass scale regulating the spread in the transverse plane of ψ_L . The explicit form of the \mathbf{p}_T dependent part follows from the assumption that in the transverse plane the valence quarks lay in a s-wave state. Such a claim is supported by the fact that one is assuming the two partons to be close, thus limiting the contributions from states with higher angular momentum. The x -dependent function $G_L(x)$ is described by a Gegenbauer polynomials expansion [80]:

$$G_L(x) = \left(1 + B_L^{(2)} C_2^{3/2} (2x - 1) + \dots\right). \quad (5)$$

The parameters $B_L^{(n)}$ regulate the longitudinal momentum distribution among the partons. By integrating over the transverse momentum \mathbf{p}_T down to the scale μ , i.e. up to distances $\sim 1/Q$, one obtains the following expression for the DA function:

$$\begin{aligned} \phi_L(x, \mu) &\propto \beta_L A_L \sqrt{x(1-x)} G_L(x, \mu) \\ &\times \left(\text{Erf} \left[\sqrt{\frac{m_q^2 + \mu^2}{8\beta_L^2 x(1-x)}} \right] - \text{Erf} \left[\sqrt{\frac{m_q^2}{8\beta_L^2 x(1-x)}} \right] \right). \end{aligned} \quad (6)$$

where now the Gegenbauer polynomials get multiplied by scale dependent momenta $B_L^{(n)}(\mu)$, see for example Ref. [81–83]. The resulting DA, $\phi_L(x, \mu)$ describing the light meson’s quark momenta distribution is typically approximated by the symmetric function [51–53]:

$$\phi_L(x) \propto x(1-x). \quad (7)$$

Having worked through the computation for a light meson, it is instructive to consider also the case of a heavy one. Here, one has to substitute the argument of the exponential in Eq.(4) accordingly:

$$\frac{\mathbf{p}_T^2 + m_q^2}{8\beta_L^2(1-x)x} \rightarrow \frac{\mathbf{p}_T^2 + m_q^2}{8\beta_H^2(1-x)} + \frac{\mathbf{p}_T^2 + m_Q^2}{8\beta_H^2 x}, \quad (8)$$

where q and Q are the light and heavy partons in the meson. The resulting DA, $\phi_H(x, \mu)$, describing the heavy meson’s quark momenta distribution can be approximated by [53]:

$$\phi_H(x) \propto \left[\frac{\xi^2}{1-x} + \frac{1}{x} - 1 \right]^{-2}, \quad (9)$$

where ξ is a small parameter of $O(m_q/m_Q)$, measuring the light/heavy parton asymmetry in the momentum distribution. The DA functions in Eqs. (7) and (9) are assumed as an ansatz for describing light and heavy meson [51, 71, 84] momentum distributions³. To simplify analytical expressions, it is often useful to consider the “very heavy” meson limit [85] by defining the parton masses $m_q = \xi M_I$, $m_Q = (1 - \xi) M_I$ and assuming the simplified expression

$$\phi_H(x) \approx \delta(1 - x - \xi) \quad (10)$$

³A detailed discussion on how adapt this DA description to the Kaon sector can be found in [24].

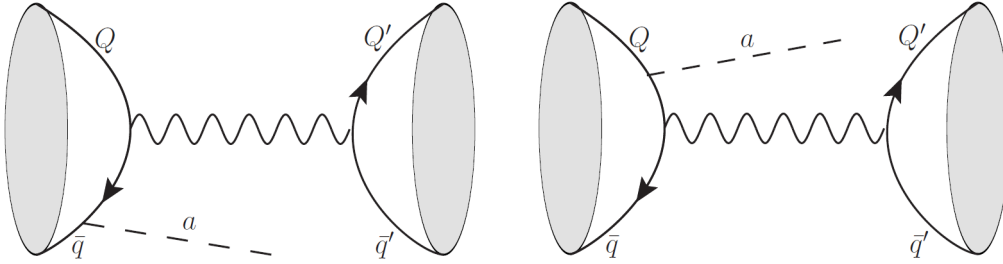


Figure 3: Tree-level s-channel of a charged $(\bar{q}Q)$ -meson decaying into a charged $(\bar{Q}'q')$ meson and an ALP. Diagrams where the ALP is emitted from the final state meson can be easily obtained.

for the DA function.

Finally one associates to mesons a spinorial representation through the Bethe-Salpeter wave function, $\Psi(x)$, that carries the quantum numbers of the resonance [20, 51, 53, 86]. Therefore, for pseudoscalar and vector meson one defines respectively:

$$\Psi_{\mathcal{P}}(x) = \frac{\phi(x)}{4} \gamma^5 (\not{P}_{\mathcal{P}} + g_{\mathcal{P}}(x) M_{\mathcal{P}}), \quad (11)$$

$$\Psi_{\mathcal{V}}(x) = \frac{\phi(x)}{4} (\sigma^{\alpha\beta} P_{\mathcal{V}\beta} - i g_{\mathcal{V}}(x) M_{\mathcal{V}} \gamma^{\alpha}) \epsilon_{\alpha}(P_{\mathcal{V}}), \quad (12)$$

The mass functions $g_{\mathcal{P},\mathcal{V}}(x)$ introduced in Eqs. (11) and (12), are typically assumed to be constant and respectively $g_H \approx 1$ and $g_L \ll 1$ for heavy or light mesons.

With all the ingredients in hand, the hadronic S-matrix elements describing meson decays in ALP can be calculated.

3 Mesonic Decay amplitudes

In this section, the amplitudes for the hadronic and leptonic meson decays into an invisible ALP are derived. The calculation of the tree-level amplitudes is performed through the Brodsky–Lepage method, while the hadronization of penguin contributions will make use of form factors calculated via LQCD methods.

3.1 Factorization for s-channel processes

A typical s-channel hadronic meson decay process in ALP is shown in Fig. 3. Looking at the picture the factorization naturally emerges: the amplitude is a product of two uncorrelated vector currents obtained by cutting the diagram along the weak boson leg connecting the hadronic external states. Let the initial mesonic state be constituted

by the $\bar{q}Q$ quark pair and the final one by the $\bar{Q}'q'$ quarks. The resulting amplitude will be of the form

$$\langle M_F | (\bar{Q}'\Gamma^{(F)\mu}q') | 0 \rangle \langle 0 | (\bar{q}\Gamma_\mu^{(I)}Q) | M_I \rangle, \quad (13)$$

where M_I and M_F are the initial and final mesons and the index I (F) indicates that the ALP is emitted from the initial (final) meson quarks. The hadronic to vacuum matrix element is defined as

$$\langle 0 | (\bar{q}\Gamma_\mu Q) | M \rangle = if_M \int dx \text{Tr}[\Psi_M(x)\Gamma_\mu]. \quad (14)$$

Note that Eqs. (11), (12) and (14) follow a slightly different notation with respect to the referred literature. In particular the functions $\phi(x)$ have been normalized to one, in such a way that in Eq. (14) the mesonic decay constants can be explicitly factorized. Moreover, the color structure, being trivial in all our processes, has been already explicitly traced. If one of the two operator $\Gamma^{(I,F)}$ in Eq. (13) is either $\gamma^\mu\gamma^5$ or γ^μ , the hadronization procedure given by Eq. (14) reproduces the usual definitions

$$\langle 0 | \bar{q}\gamma^\mu\gamma_5 Q | \mathcal{P}(P_{\mathcal{P}}) \rangle = if_{\mathcal{P}}P_{\mathcal{P}}^\mu, \quad (15)$$

$$\langle 0 | \bar{q}\gamma^\mu Q | \mathcal{V}(P_{\mathcal{V}}) \rangle = f_{\mathcal{V}}M_{\mathcal{V}}\epsilon^\mu(P_{\mathcal{V}}), \quad (16)$$

for pseudoscalar and vector mesons, respectively. Thanks to the decorrelation between final and initial state one can obtain leptonic and radiative decay contributions by simply replacing one of the hadronic currents in Eq. (13) with a leptonic one.

The full amplitude for an s-channel W-mediated hadronic tree level meson decay can be written as:

$$\langle M_F | (\bar{Q}'\gamma^\mu P_L q') | 0 \rangle \langle 0 | (\bar{q}\Gamma_\mu^{(I)}Q) | M_I \rangle + \langle M_F | (\bar{Q}'\Gamma_\mu^{(F)}q') | 0 \rangle \langle 0 | (\bar{q}\gamma^\mu P_L Q) | M_I \rangle. \quad (17)$$

Note that the diagram where the ALP is emitted from the W internal line automatically vanishes, being the W^+W^- -ALP coupling proportional to the fully antisymmetric 4D tensor. The initial and finale Dirac structures, $\Gamma_\mu^{(I,F)}$, can be extracted from the corresponding Feynman diagrams In Fig. 3 only the case of initial meson ALP emission is shown explicitly, with the final meson emission case obtainable straightforwardly. The initial and final hard-scattering amplitudes read respectively:

$$\begin{aligned} \Gamma_\mu^{(I)} &= \frac{4G_F}{\sqrt{2}f_a} V_{CKM} \left(c_q m_q \frac{\gamma^5 \not{k} \gamma_\mu P_L}{m_a^2 - 2k \cdot P_q} - c_Q m_Q \frac{\gamma_\mu P_L \not{k} \gamma^5}{m_a^2 - 2k \cdot P_Q} \right) \\ \Gamma_\mu^{(F)} &= \frac{4G_F}{\sqrt{2}f_a} V_{CKM} \left(c_{Q'} m_{Q'} \frac{\gamma^5 \not{k} \gamma_\mu P_L}{m_a^2 + 2k \cdot P_{Q'}} - c_{q'} m_{q'} \frac{\gamma_\mu P_L \not{k} \gamma^5}{m_a^2 + 2k \cdot P_{q'}} \right), \end{aligned} \quad (18)$$

with k^μ the ALP 4-momentum. For example, the amplitude for the pseudoscalar-to-pseudoscalar decay, with the ALP emitted from the initial meson, arising from the second term in Eq. (17), reads:

$$\langle \mathcal{P}_F | (\bar{Q}' \gamma^\mu P_L q') | 0 \rangle \langle 0 | (\bar{q} \Gamma_\mu^{(1)} Q) | \mathcal{P}_I \rangle = i \frac{f_{\mathcal{P}_F}}{2} P_F^\mu \left(i f_{\mathcal{P}_I} \int dx \text{Tr} [\Psi_{\mathcal{P}_I}(x) \Gamma_\mu^{(1)}] \right). \quad (19)$$

The case of vector mesons can be straightforwardly obtained by using Eqs. (12) and (16) instead of Eqs. (11) and (15) in the corresponding amplitudes. In the following subsections the explicit expression for the various hadronic and leptonic s-channels decays are presented.

3.1.1 Mesonic decays

Using Eqs. (14), (18) and (19) and defining $P_q = (1-x)P_I$, $P_Q = xP_I$, $P_{q'} = (1-y)P_F$ and $P_{Q'} = yP_F$, the s-channel amplitudes for a pseudoscalar-to-pseudoscalar meson decay, exemplified by the $B \rightarrow Ka$ decay, with the ALP radiated from the initial (I) or final (F) meson read:

$$\begin{aligned} \mathcal{A}_I^{(s)} &= \frac{G_F V_{CKM} f_I f_F (k \cdot P_F)}{\sqrt{2} f_a} M_I \\ &\int_0^1 dx g_I(x) \left[\frac{c_q m_q \theta(1-x-\delta_a^M)}{m_a^2 - 2k \cdot P_I(1-x)} - \frac{c_Q m_Q \theta(x-\delta_a^M)}{m_a^2 - 2k \cdot P_I x} \right] \phi_I(x) \end{aligned} \quad (20)$$

$$\begin{aligned} \mathcal{A}_F^{(s)} &= \frac{G_F V_{CKM} f_I f_F (k \cdot P_I)}{\sqrt{2} f_a} M_F \\ &\int_0^1 dy g_F(y) \left[\frac{c_{Q'} m_{Q'}}{m_a^2 + 2k \cdot P_F y} - \frac{c_{q'} m_{q'}}{m_a^2 + 2k \cdot P_F(1-y)} \right] \phi_F(y). \end{aligned} \quad (21)$$

In the integrals of Eq. (20) an explicit cut-off, $\delta_a^M = m_a/(2M_I)$, has to be introduced for $m_a \neq 0$ to remove the unphysical singularities. A simplified analytical expression of the amplitudes of Eq. (20–21) can be obtained by taking $m_a = 0$ and considering the “very heavy” meson limit defined in Eq. (10):

$$\left| \mathcal{A}_I^{(s)} \right| \approx \frac{G_F V_{CKM} f_I f_F}{2\sqrt{2} f_a} M_I^2 g_H(c_q - c_Q) \quad (22)$$

$$\left| \mathcal{A}_F^{(s)} \right| \approx \frac{G_F V_{CKM} f_I f_F}{2\sqrt{2} f_a} M_F^2 g_H(c_{Q'} - c_{q'}), \quad (23)$$

where g_H is assumed to be constant. This approximation clearly shows the $M_{I(F)}^2$ dependence of the ISR (FSR) amplitude. Therefore, in typical pseudoscalar-to-pseudoscalar meson decays the ALP is predominantly emitted from the initial meson. Moreover, as pointed out in [24], a parametric cancellation occurs in the universal ALP-fermion coupling scenario. This cancellation is still partially at work even when the full $\phi(x)$ is used and indicates a possible underestimation of the amplitudes when $c_{q(q')} = c_{Q(Q')}$ is chosen.

The s-channel amplitudes for a pseudoscalar-to-vector meson decay, exemplified by the $B \rightarrow K^* a$ decay, with the ALP radiated from the initial (I) and final (F) meson read:

$$\mathcal{B}_I^{(s)} = i \frac{G_F V_{CKM} f_I f_F (k \cdot \epsilon(P_F))}{\sqrt{2} f_a} M_I M_F \int_0^1 dx g_I(x) \left[\frac{c_q m_q \theta(1-x-\delta_a^M)}{m_a^2 - 2k \cdot P_I(1-x)} - \frac{c_Q m_Q \theta(x-\delta_a^M)}{m_a^2 - 2k \cdot P_I x} \right] \phi_I(x) \quad (24)$$

$$\mathcal{B}_F^{(s)} = i \frac{G_F V_{CKM} f_I f_F \epsilon^\alpha(P_F) P_F^\beta (k^\beta P_I^\alpha - k^\alpha P_I^\beta)}{\sqrt{2} f_a} \int_0^1 dy \left[\frac{c_{Q'} m_{Q'}}{m_a^2 + 2k \cdot P_F y} - \frac{c_{q'} m_{q'}}{m_a^2 + 2k \cdot P_F(1-y)} \right] \phi_F(y), \quad (25)$$

where ϵ^α is the polarization of the vector resonance. The results for vector-to-pseudoscalar meson decay read:

$$\mathcal{C}_I^{(s)} = -i \frac{G_F V_{CKM} f_I f_F \epsilon^\alpha(P_I) P_I^\beta (k^\alpha P_F^\beta - k^\beta P_F^\alpha)}{\sqrt{2} f_a} \int_0^1 dx \left[\frac{c_q m_q \theta(1-x-\delta_a^M)}{m_a^2 - 2k \cdot P_I(1-x)} - \frac{c_Q m_Q \theta(x-\delta_a^M)}{m_a^2 - 2k \cdot P_I x} \right] \phi_I(x). \quad (26)$$

$$\mathcal{C}_F^{(s)} = -i \frac{G_F V_{CKM} f_I f_F (k \cdot \epsilon(P_F))}{\sqrt{2} f_a} M_I M_F \int_0^1 dy g_F(y) \left[\frac{c_{Q'} m_{Q'}}{m_a^2 + 2k \cdot P_F y} - \frac{c_{q'} m_{q'}}{m_a^2 + 2k \cdot P_F(1-y)} \right] \phi_F(y). \quad (27)$$

One can easily show that also in these cases, for $m_a = 0$ and assuming the “very heavy” meson limit, simple expressions for the amplitudes of the \mathcal{B} and \mathcal{C} -type decays can be recovered, exhibiting a meson $M_{I(F)}^2$ dependence and a parametric cancellation for a universal ALP-fermion coupling, similarly to the results of Eqs. (22–23).

Finally the amplitudes for vector-to-vector meson decays read:

$$\begin{aligned}
\mathcal{D}_I^{(s)} = & -i \frac{G_F V_{CKM} f_I f_F}{\sqrt{2} f_a} \epsilon^\alpha(P_I) \epsilon^\mu(P_F) P_I^\beta M_F \\
& \int_0^1 dx \left[\frac{c_q m_q \theta(1-x-\delta_a^M)}{m_a^2 - 2k \cdot P_I (1-x)} (\varepsilon_{\alpha\beta\mu\rho} k^\rho + ik^\beta g^{\alpha\mu} - ik^\alpha g^{\beta\mu}) + \right. \\
& \left. + \frac{c_Q m_Q \theta(x-\delta_a^M)}{m_a^2 - 2k \cdot P_I x} (\varepsilon_{\alpha\beta\mu\rho} k^\rho + ik^\alpha g^{\beta\mu} - ik^\beta g^{\alpha\mu}) \right] \phi_I(x) \quad (28)
\end{aligned}$$

$$\begin{aligned}
\mathcal{D}_F^{(s)} = & -i \frac{G_F V_{CKM} f_I f_F}{\sqrt{2} f_a} \epsilon^\alpha(P_F) \epsilon^\mu(P_I) P_F^\beta M_I \\
& \int_0^1 dy \left[\frac{c_{q'} m_{q'}}{m_a^2 + 2k \cdot P_F y} (\varepsilon_{\alpha\beta\mu\rho} k^\rho + ik^\beta g^{\alpha\mu} - ik^\alpha g^{\beta\mu}) + \right. \\
& \left. + \frac{c_{Q'} m_{Q'}}{m_a^2 + 2k \cdot P_F (1-y)} (\varepsilon_{\alpha\beta\mu\rho} k^\rho + ik^\alpha g^{\beta\mu} - ik^\beta g^{\alpha\mu}) \right] \phi_F(y). \quad (29)
\end{aligned}$$

In the “very heavy” meson limit the vector-to-vector amplitudes read:

$$\left| \mathcal{D}_I^{(s)} \right| \approx \frac{f_I f_F G_F M_I^2 V_{CKM}}{4 f_a} \sqrt{(c_Q - c_q)^2 + 4 \frac{M_F^2}{M_I^2} (c_Q^2 + c_q^2)}, \quad (30)$$

$$\left| \mathcal{D}_F^{(s)} \right| \approx \frac{f_I f_F G_F M_F^2 V_{CKM}}{4 f_a} \sqrt{(c'_Q - c'_q)^2 + 4 \frac{M_I^2}{M_F^2} (c'_Q{}^2 + c'_q{}^2)}. \quad (31)$$

The parametric cancellation in this case is not completely at work as the epsilon tensor in Eqs. (28-29) introduces an extra term proportional to the sum of the couplings squared. Notice also that, in the universal ALP-fermion coupling scenario, both the ISR and FSR amplitudes get proportional to the product $M_I M_F$ and there is no clear suppression of the FSR ALP process with respect to the ISR one, contrary to what happens for all the processes described by the \mathcal{A} , \mathcal{B} and \mathcal{C} amplitudes.

3.1.2 Leptonic decay

For completeness we report here, briefly, the semileptonic meson decays, $M \rightarrow \ell \nu_\ell a$, derived in details in [25]. In Fig. 4 the diagrams where the ALP is emitted from the meson are drawn. The diagrams where the ALP is emitted by the charged leptons follow straightforwardly. These amplitudes can be factorized as

$$\langle 0 | (\bar{q} \Gamma_\mu^{(h)} Q) | M \rangle (\bar{\ell} \gamma^\mu P_L \nu) + \langle 0 | (\bar{q} \gamma^\mu P_L Q) | M \rangle (\bar{\ell} \Gamma_\mu^{(\ell)} \nu), \quad (32)$$

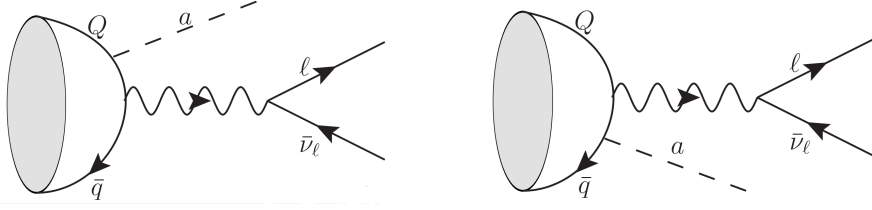


Figure 4: Tree level contributions to the $M \rightarrow \ell \nu_\ell a$ amplitude, with the ALP emitted from the M meson. The diagram where the ALP is emitted from the charged lepton is straightforward.

with $\Gamma_\mu^{(h)}$ and $\Gamma_\mu^{(\ell)}$ the Dirac structures related to the hadronic and leptonic emission, respectively. Using the methods introduced in Eqs. (14–15) one obtains

$$\mathcal{E}_h = \frac{4iG_F V_{CKM} f_M}{\sqrt{2}} \frac{M_M^2}{f_a 2k \cdot P_M} \left[c_Q \frac{m_Q}{M_M} \Phi_M^{(Q)}(m_a^2) - c_q \frac{m_q}{M_M} \Phi_M^{(q)}(m_a^2) \right] (\bar{\ell} \not{k} P_L \nu_\ell). \quad (33)$$

for the amplitudes associated to the hadronic ALP emission. The functions $\Phi_M^{(q,Q)}(m_a^2)$ contain the integrals over the quark momentum fraction and are given by:

$$\begin{aligned} \Phi_M^{(q)}(m_a^2) &= \int_0^{1-\delta_M} \frac{k \cdot P_M}{m_a^2 - 2(1-x)k \cdot P_M} \phi_M(x) g_M(x) dx \\ \Phi_M^{(Q)}(m_a^2) &= \int_{\delta_M}^1 \frac{k \cdot P_M}{m_a^2 - 2xk \cdot P_M} \phi_M(x) g_M(x) dx. \end{aligned} \quad (34)$$

One can obtain a simple expression for the hadronic amplitude by employing the “very heavy” meson approximation discussed in Sec. 3.1.1. For $m_a = 0$ one has

$$\mathcal{E}_h \approx iG_F V_{CKM} \frac{f_M}{\sqrt{2}f_a} \frac{M_M^2}{k \cdot P_M} (c_q - c_Q) (\bar{\ell} \not{k} P_L \nu_\ell). \quad (35)$$

The leptonic decay amplitude for the lepton ALP–emission process can be easily obtained by using the definition of the meson form factors of Eq. (15), giving

$$\mathcal{E}_\ell = -\frac{4iG_F}{\sqrt{2}} V_{qQ} \frac{f_M}{f_a} \left[c_\ell m_\ell (\bar{\ell} P_L \nu_\ell) - \frac{c_\ell m_\ell^2}{m_a^2 + 2k \cdot p_\ell} (\bar{\ell} \not{k} P_L \nu_\ell) \right]. \quad (36)$$

assuming vanishing neutrino masses.

3.2 Factorization of t –channel processes

Following a similar approach to the one used in the previous subsection one can now study meson decays occurring through a t –channel W exchange. In Fig. 5, typical

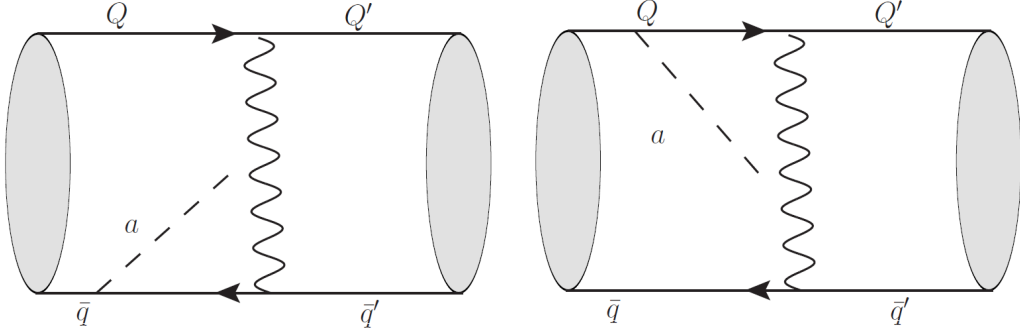


Figure 5: Tree-level t -channel of a neutral $(\bar{q}Q)$ -meson decaying into a neutral $(\bar{Q}'q')$ meson and an ALP. Diagrams where the ALP is emitted from the final state meson can be easily obtained. Similar diagrams can be depicted for the CP conjugate process.

diagrams with the ALP emitted from the initial meson state are depicted. Once again, diagrams with the ALP emitted from the final state are obvious, while the diagram where the ALP is emitted from the W internal line automatically vanishes. In this case the hadronic process can be written:

$$\langle M_F | (\bar{Q}' \Gamma_\mu^{(Q)} Q) (\bar{q} \gamma^\mu P_L q') | M_I \rangle + \langle M_F | (\bar{Q}' \gamma^\mu P_L Q) (\bar{q} \Gamma_\mu^{(\bar{q})} q') | M_I \rangle, \quad (37)$$

where $\Gamma_\mu^{(Q,\bar{q})}$ are the Feynman amplitudes corresponding to the ALP emission from a quark or an antiquark line. Note that for processes in the t -channel, there are no trivial mesonic currents representing either the initial or final meson, and then the full Brodsky–Lepage machinery is always required for calculating these amplitudes. The tree-level hard scattering of the diagrams depicted in Fig.5, gives:

$$\Gamma_\mu^{(Q)} = \frac{4G_F}{\sqrt{2}f_a} V_{CKM} \left(c_{Q'} m_{Q'} \frac{\gamma^5 \not{k} \gamma_\mu P_L}{m_a^2 + 2k \cdot P_{Q'}} - c_Q m_Q \frac{\gamma_\mu P_L \not{k} \gamma^5}{m_a^2 - 2k \cdot P_Q} \right) \quad (38)$$

$$\Gamma_\mu^{(\bar{q})} = \frac{4G_F}{\sqrt{2}f_a} V_{CKM} \left(c_q m_q \frac{\gamma^5 \not{k} \gamma_\mu P_L}{m_a^2 - 2k \cdot P_q} - c_{q'} m_{q'} \frac{\gamma_\mu P_L \not{k} \gamma^5}{m_a^2 + 2k \cdot P_{q'}} \right). \quad (39)$$

Using the procedure described in Ref. [53], one obtains, for the t -channel factorization:

$$\begin{aligned} \langle M_F | (\bar{Q}' \Gamma_\mu^{(Q)} Q) (\bar{q} \gamma^\mu P_L q') | M_I \rangle &= -\frac{f_{M_F} f_{M_I}}{\sqrt{2}} \int dx dy \text{Tr} [\Psi_{M_I}(x) \gamma^\mu P_L \Psi_{M_F}(y) \Gamma_\mu^{(Q)}], \\ \langle M_F | (\bar{Q}' \gamma^\mu P_L Q) (\bar{q} \Gamma_\mu^{(\bar{q})} q') | M_I \rangle &= -\frac{f_{M_F} f_{M_I}}{\sqrt{2}} \int dx dy \text{Tr} [\Psi_{M_I}(x) \Gamma_\mu^{(\bar{q})} \Psi_{M_F}(y) \gamma^\mu P_L]. \end{aligned} \quad (40)$$

Substituting $\Gamma_\mu^{(Q,\bar{q})}$ according to Eqs. (38–39) one finds the hadronized amplitudes. It is then phenomenologically convenient to separate ISR and FSR amplitudes. The

pseudoscalar-to-pseudoscalar meson decay amplitudes read:

$$\begin{aligned} \mathcal{A}_I^{(t)} &= \frac{G_F V_{CKM} f_I f_F (k \cdot P_F)}{2f_a} M_I \\ &\int_0^1 dx g_I(x) \left[\frac{c_Q m_Q \theta(x - \delta_a^M)}{m_a^2 - 2k \cdot P_I x} - \frac{c_q m_q \theta(1 - x - \delta_a^M)}{m_a^2 - 2k \cdot P_I (1 - x)} \right] \phi_I(x), \end{aligned} \quad (41)$$

$$\begin{aligned} \mathcal{A}_F^{(t)} &= \frac{G_F V_{CKM} f_I f_F (k \cdot P_I)}{2f_a} M_F \\ &\int_0^1 dy g_F(y) \left[\frac{c_{q'} m_{q'}}{m_a^2 + 2k \cdot P_F (1 - y)} - \frac{c_{Q'} m_{Q'}}{m_a^2 + 2k \cdot P_F y} \right] \phi_F(y), \end{aligned} \quad (42)$$

while the pseudoscalar-to-vector t -channel transitions read:

$$\begin{aligned} \mathcal{B}_I^{(t)} &= i \frac{G_F V_{CKM} f_I f_F (k \cdot \epsilon(P_F))}{2f_a} M_I M_F \\ &\int_0^1 dx g_I(x) \left[\frac{c_Q m_Q \theta(x - \delta_a^M)}{m_a^2 - 2k \cdot P_I x} - \frac{c_q m_q \theta(1 - x - \delta_a^M)}{m_a^2 - 2k \cdot P_I (1 - x)} \right] \phi_F(x), \end{aligned} \quad (43)$$

$$\begin{aligned} \mathcal{B}_F^{(t)} &= i \frac{G_F V_{CKM} f_I f_F \epsilon^\alpha(P_F) P_F^\beta (k^\beta P_I^\alpha - k^\alpha P_I^\beta)}{2f_a} \\ &\int_0^1 dy \left[\frac{c_{Q'} m_{Q'}}{m_a^2 + 2k \cdot P_F y} - \frac{c_{q'} m_{q'}}{m_a^2 + 2k \cdot P_F (1 - y)} \right] \phi_F(y). \end{aligned} \quad (44)$$

Finally, the vector-to-pseudoscalar and vector-to-vector decays amplitudes are given by:

$$\begin{aligned} \mathcal{C}_I^{(t)} &= -i \frac{G_F V_{CKM} f_I f_F \epsilon^\alpha(P_I) P_I^\beta (k^\beta P_F^\alpha - k^\alpha P_F^\beta)}{2f_a} \\ &\int_0^1 dx \left[\frac{c_Q m_Q \theta(x - \delta_a^M)}{m_a^2 - 2k \cdot P_I x} - \frac{c_q m_q \theta(1 - x - \delta_a^M)}{m_a^2 - 2k \cdot P_I (1 - x)} \right] \phi_I(x). \end{aligned} \quad (45)$$

$$\begin{aligned} \mathcal{C}_F^{(t)} &= -i \frac{G_F V_{CKM} f_I f_F (k \cdot \epsilon(P_F))}{2f_a} M_I M_F \\ &\int_0^1 dy g_F(y) \left[\frac{c_{Q'} m_{Q'}}{m_a^2 + 2k \cdot P_F y} - \frac{c_{q'} m_{q'}}{m_a^2 + 2k \cdot P_F (1 - y)} \right] \phi_F(y), \end{aligned} \quad (46)$$

and by

$$\mathcal{D}_I^{(t)} = -i \frac{G_F V_{CKM} f_I f_F \epsilon^\alpha(P_I) \epsilon^\mu(P_F) P_I^\beta M_F}{2f_a}$$

$$\int_0^1 dx \left[\frac{c_Q m_Q \theta(x - \delta_a^M)}{m_a^2 - 2k \cdot P_I x} (\varepsilon_{\alpha\beta\mu\rho} k^\rho - ik^\beta g^{\alpha\mu} + ik^\alpha g^{\beta\mu}) + \frac{c_q m_q \theta(1 - x - \delta_a^M)}{m_a^2 - 2k \cdot P_I (1 - x)} (\varepsilon_{\alpha\beta\mu\rho} k^\rho - ik^\alpha g^{\beta\mu} + ik^\beta g^{\alpha\mu}) \right] \phi_I(x). \quad (47)$$

$$\mathcal{D}_F^{(t)} = -i \frac{G_F V_{CKM} f_I f_F}{2f_a} \epsilon^\alpha(P_I) \epsilon^\mu(P_F) P_F^\beta M_I \int_0^1 dy \left[\frac{c_{Q'} m_{Q'}}{m_a^2 + 2k \cdot P_F y} (\varepsilon_{\alpha\beta\mu\rho} k^\rho - ik^\beta g^{\alpha\mu} + ik^\mu g^{\alpha\beta}) + \frac{c_{q'} m_{q'}}{m_a^2 + 2k \cdot P_F (1 - y)} (\varepsilon_{\alpha\beta\mu\rho} k^\rho - ik^\mu g^{\alpha\beta} + ik^\beta g^{\alpha\mu}) \right] \phi_F(y). \quad (48)$$

It is interesting to note that the results derived here are very symmetric with the s -channel case, up to a sign and a factor of $\sqrt{2}$. The only exception is given by the vector-to-vector decays where a minus sign is present in parts of the tensor structure w.r.t. the s -channel case. One can apply the ‘‘very heavy’’ approximation used in Sec. 3.1.1 to derive simple analytic results also for the t -channel amplitudes. Expressions similar to the ones shown in Eqs. (22–23) and Eqs. (30–31) can be obtained also in the t -channel case.

3.3 Penguin Hadronization

Flavor changing neutral current meson decays in ALP will often receive the dominant contributions from the one-loop penguin diagrams [21, 44, 87], shown in Fig. 6. In

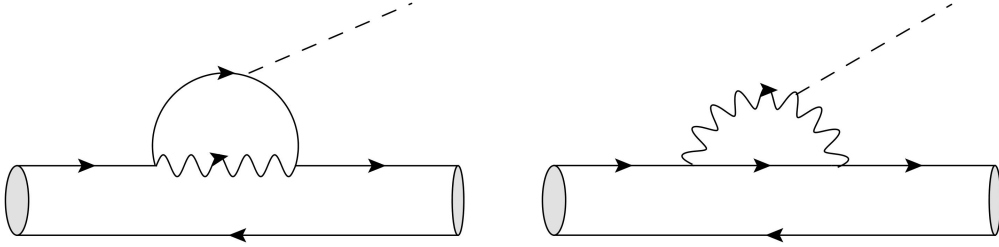


Figure 6: Dominant one-loop penguin contributions to meson decay in ALP.

this kind of processes, only one quark line participates actively to the ALP emission, with the other quark playing the role of spectator.

The hadronic matrix element for pseudoscalar-to-pseudoscalar meson decays is mediated by a vector current customarily factorised as:

$$\langle \mathcal{P}_F | \bar{q} \gamma^\mu Q | \mathcal{P}_I \rangle = f_+(k^2) (P_I + P_F)^\mu + f_-(k^2) k^\mu \quad (49)$$

with $k = P_I - P_F$. The $f_{+,-}(k^2)$ form factors can be obtained from LQCD calculations [50, 88–97], and are transition specific. Using Eq. (49), the penguin contribution to the $\mathcal{P}_I \rightarrow \mathcal{P}_F a$ decay amplitude, assuming flavor diagonal quarks-ALP couplings, reads:

$$\mathcal{G}_{\mathcal{P}_I \rightarrow \mathcal{P}_F} = \frac{G_F m_q^2 M_I^2}{2\sqrt{2}\pi^2 f_a} \left(1 - \frac{M_F^2}{M_I^2}\right) \left[f_+(k^2) + \frac{k^2}{M_I^2 - M_F^2} f_-(k^2) \right] \sum_f c_{ij}^{(f)}. \quad (50)$$

The coefficient $c_{ij}^{(f)}$ has been opportunely normalized to factorize out the heaviest quark mass running in the loop, here dubbed m_q , and is defined as:

$$c_{ij}^{(f)} = V_{fi} V_{fj}^* \left[3 c_W \frac{g(x_f)}{x_q} - \frac{c_f x_f}{4 x_q} \ln \left(\frac{f_a^2}{m_f^2} \right) \right] \quad \text{with} \quad \left(x_f \equiv \frac{m_f^2}{m_W^2} \right). \quad (51)$$

The penguin contribution where the ALP emitted from the internal W line is included here for completeness, even if in the following phenomenological analysis $c_W = 0$ will be assumed⁴. One-loop diagrams, with the ALP emitted from the initial/final quarks are suppressed by at least an extra m_f^2/m_W^2 factor (being m_f the mass of the initial/final quark) with respect to the penguin contributions, as they arise at third order in the external momenta expansion. In the case of the K and D meson they can be safely neglected even compared to the tree level contributions. For B mesons, instead, these contributions are roughly of the same order of the tree-level ones. Therefore, the complete 1-loop renormalization should be performed to be able to extract information on the ALP-external fermion couplings.

In the case of vector-to-pseudoscalar transitions the hadronic matrix element can be divided in terms of four independent form factors. See for example [90] for the general expression. For the specific type of decays considered here, the only surviving form factor is given by:

$$\langle \mathcal{P} | \bar{q} \gamma^\mu \gamma_5 Q | \mathcal{V} \rangle = 2 i M_{\mathcal{V}} A_0(k^2) \frac{(\epsilon(P_{\mathcal{V}}) \cdot k) k^\mu}{k^2}. \quad (52)$$

For numerical evaluation the $A_0(k^2)$ results explicitly reported in [88–90, 92–94, 98–101] has been used. For strange meson decays, when not available, the form factors have been chosen to be 1, assuming an exact $SU(3)$ flavor symmetry. Finally, following the conventions of [99], one obtains

$$\mathcal{G}_{\mathcal{V} \rightarrow \mathcal{P}} = i \frac{G_F m_q^2}{\sqrt{2}\pi^2 f_a} M_{\mathcal{V}} A_0(k^2) (\epsilon(P_{\mathcal{V}}) \cdot k) \sum_f c_{ij}^{(f)} \quad (53)$$

⁴The contribution due to weak boson-ALP coupling and the interplay between quark and weak boson ALP coupling has been considered for example in [21].

with m_q the mass of the heaviest quark running in the loop and the coefficient $c_{ij}^{(f)}$ defined previously in Eq. (51). The case of vector-to-pseudoscalar can be obtained from Eq. (53) by exchanging M_V with M_P and taking the conjugate of the amplitude.

4 Phenomenology of Invisible ALP and Mesons

From the meson decay amplitudes calculated in the previous section, stringent limits on the ALP-fermion Effective Lagrangian of Eq. (2) can now be derived. The two different classes of meson decays are going to be discussed separately. Hadronic meson decays in ALPs are expected in general, to be the most constraining processes to test ALP–quark couplings in the sub-GeV ALP mass range, mainly thanks to the high precision experimental results of the Kaon sector [54–58]. Nonetheless, very promising results are expected from B –factories [59–65], for ALP masses up to few GeV [21, 23, 44, 102]. Semileptonic decays, on the other hand are useful to test ALP–lepton couplings producing new bounds in the KeV–GeV range for the all the ALP–charged lepton couplings, whereas most of the limits on ALP–quark couplings are not competitive with the ones obtained from the hadronic decay channels.

4.1 Hadronic final states

In Sec. 3 the tree-level and one-loop (penguin) contributions to the hadronic meson decays into an invisible ALP, $M_I \rightarrow M_F a$, have been derived. In Tab. 1 the amplitudes of several charged meson decays are collected. For definiteness, $m_a = 0$, $f_a = 1$ TeV and $c_f = \pm 1$ have been used. As noticed in Sec. 3.1 and 3.2, accidental cancellation can occur in the tree-level amplitudes, depending on the relative sign between $c_{Q^{(\prime)}}$ and $c_{q^{(\prime)}}$ for all the processes but vector-to-vector decays, see Eqs. (20–27) and Eqs. (41–46). To make evident the impact of this accidental cancellation, the tree-level results in Tab. 1 has been shown with a (*min* – *max*) interval, obtained by setting $c_{Q^{(\prime)}}/c_{q^{(\prime)}} = (+1, -1)$ respectively. The origin of this parametric cancellation has been proved analytically by [24] both in the “very light” and “very heavy” meson limit. In Sec. 3.1 the results for the “very heavy” meson limits have been explicitly shown for the \mathcal{A} -type decays. From the results of Tab. 1, one learns which is the effectiveness of this parametric cancellation, once the numerical integration is performed using the non-approximated heavy DA function of Eq. (9). Depending on the specific decay channel, the tree-level decay rate can change from one to two orders of magnitude. Notice that in Tab. 1 no vector-to-vector decay is presented, being still experimentally marginal.

It is also useful to note from Eqs. (22) and (23) that the ratio between the tree-level ISR and FSR amplitudes is always independent of the particular nature of the

Channel	Tree-Level	Penguin
$B_c^\pm \rightarrow D_s^\pm a$	$(6 - 160) \times 10^{-11}$	2×10^{-6}
$B_c^\pm \rightarrow D^\pm a$	$(1 - 30) \times 10^{-11}$	3×10^{-7}
$B_c^\pm \rightarrow K^{*\pm} a$	$(2 - 70) \times 10^{-11}$	n.a.
$B_c^\pm \rightarrow \rho^\pm a$	$(4 - 100) \times 10^{-11}$	n.a.
$B_c^\pm \rightarrow K^\pm a$	$(8 - 230) \times 10^{-12}$	n.a.
$B_c^\pm \rightarrow \pi^\pm a$	$(3 - 85) \times 10^{-11}$	n.a.
$B^\pm \rightarrow D_s^\pm a$	$(5 - 30) \times 10^{-12}$	n.a.
$B^\pm \rightarrow D^\pm a$	$(1 - 7) \times 10^{-12}$	n.a.
$B^\pm \rightarrow K^{*\pm} a$	$(1 - 7) \times 10^{-12}$	4×10^{-6}
$B^\pm \rightarrow \rho^\pm a$	$(3 - 20) \times 10^{-12}$	4×10^{-7}
$B^\pm \rightarrow K^\pm a$	$(8 - 50) \times 10^{-13}$	2×10^{-6}
$B^\pm \rightarrow \pi^\pm a$	$(3 - 20) \times 10^{-12}$	3×10^{-7}
$D_s^\pm \rightarrow K^{*\pm} a$	$(1 - 60) \times 10^{-11}$	6×10^{-12}
$D_s^\pm \rightarrow \rho^\pm a$	$(3 - 170) \times 10^{-11}$	n.a.
$D_s^\pm \rightarrow K^\pm a$	$(6 - 300) \times 10^{-12}$	7×10^{-12}
$D_s^\pm \rightarrow \pi^\pm a$	$(2 - 120) \times 10^{-11}$	n.a.
$D^\pm \rightarrow K^{*\pm} a$	$(2 - 100) \times 10^{-12}$	n.a.
$D^\pm \rightarrow \rho^\pm a$	$(7 - 290) \times 10^{-12}$	3×10^{-12}
$D^\pm \rightarrow K^\pm a$	$(1 - 50) \times 10^{-12}$	n.a.
$D^\pm \rightarrow \pi^\pm a$	$(5 - 200) \times 10^{-12}$	6×10^{-12}
$K^{*\pm} \rightarrow K^\pm a$	$(5 - 25) \times 10^{-13}$	4×10^{-8}
$K^{*\pm} \rightarrow \pi^\pm a$	$(3 - 20) \times 10^{-12}$	3×10^{-9}
$\rho^\pm \rightarrow K^\pm a$	$(8 - 25) \times 10^{-12}$	2×10^{-9}
$\rho^\pm \rightarrow \pi^\pm a$	$(3 - 9) \times 10^{-11}$	4×10^{-10}
$K^\pm \rightarrow \pi^\pm a$	$(2 - 10) \times 10^{-12}$	5×10^{-10}

Table 1: Tree-level and penguin contribution to the hadronic charged meson decay rates, calculated for $m_a = 0$, $f_a = 1$ TeV and $c_f = \pm 1$, expressed in GeV^{-1} units. The interval in the tree-level column is obtained by setting $c_Q/c_q = (1, -1)$.

decay (s or t) and, with the only exception of the vector to vector meson decay, is given by:

$$R_{I/F}^T = \left| \frac{\mathcal{M}_I^{(s,t)}}{\mathcal{M}_F^{(s,t)}} \right| \simeq \left(\frac{M_I}{M_F} \right)^2, \quad (54)$$

with the identity strictly holding in the ALP massless limit and assuming a “very light” or a “very heavy” DA function. Therefore, for all the corresponding processes,

Channel	Tree-Level	Penguins
$B_s^0 \rightarrow D_s^0 a$	n.a.	4×10^{-7}
$B_s^0 \rightarrow D^0 a$	$(7 - 70) \times 10^{-12}$	n.a.
$B_s^0 \rightarrow K^{*0} a$	n.a.	4×10^{-6}
$B_s^0 \rightarrow \rho^0 a$	$(4 - 50) \times 10^{-13}$	n.a.
$B_s^0 \rightarrow K_L^0 a$	n.a.	3×10^{-7}
$B^0 \rightarrow K^{*0} a$	n.a.	4×10^{-6}
$B^0 \rightarrow D^0 a$	$(3 - 30) \times 10^{-11}$	n.a.
$B^0 \rightarrow \rho^0 a$	$(2 - 20) \times 10^{-12}$	6×10^{-7}
$B^0 \rightarrow K_L^0 a$	n.a.	4×10^{-6}
$B^0 \rightarrow \pi^0 a$	$(1 - 10) \times 10^{-12}$	5×10^{-7}
$D^0 \rightarrow K^{*0} a$	$(7 - 300) \times 10^{-12}$	n.a.
$D^0 \rightarrow \rho^0 a$	$(5 - 200) \times 10^{-12}$	4×10^{-12}
$D^0 \rightarrow K_L^0 a$	$(7 - 270) \times 10^{-13}$	n.a.
$D^0 \rightarrow \pi^0 a$	$(2 - 100) \times 10^{-12}$	3×10^{-12}
$K^{*0} \rightarrow K^0 a$	$(2 - 6) \times 10^{-12}$	3×10^{-9}
$K^{*0} \rightarrow \pi^0 a$	$(1 - 2) \times 10^{-11}$	3×10^{-9}
$\rho^0 \rightarrow K^0 a$	$(1 - 3) \times 10^{-11}$	2×10^{-9}
$\rho^0 \rightarrow \pi^0 a$	$(2 - 7) \times 10^{-11}$	3×10^{-9}
$K_L^0 \rightarrow \pi^0 a$	$(4 - 20) \times 10^{-15}$	1×10^{-10}

Table 2: Tree-level and penguin contribution to the hadronic neutral meson decay rates, calculated for $m_a = 0$, $f_a = 1$ TeV and $c_f = \pm 1$, expressed in GeV^{-1} units. The interval in the tree-level column is obtained by setting $c_Q/c_q = (1, -1)$.

the decay amplitude is always dominated by the ISR ALP emission. Finally, in Tab. 1, both the tree-level and penguin contributions, when available, are presented. As a rule of thumb the tree-level vs one-loop amplitudes ratio can be estimated by:

$$R_{T/L} = \left| \frac{\mathcal{M}_T^{(s,t)}}{\mathcal{M}_L} \right| \approx 2\pi^2 \frac{f_I f_F}{m_f^2} \left| \frac{V_T^{\text{CKM}}}{V_L^{\text{CKM}}} \right|, \quad (55)$$

where m_f is the mass of the heaviest quark running in the penguin and $f_{I,F}$ the initial and final meson decay constants. Notice that for most of the D decays the tree-level contribution is comparable if not larger than the loop one, as clearly the m_b^2 penguin loop enhancement is not sufficient to compensate for the typical loop suppression factor. Conversely, for the K and B meson sector the tree/loop ratio looks really tiny thanks to the large m_t^2 penguin enhancement. Nevertheless, for the K sector the

tree-level diagrams may have a non negligible impact, as they depend on different, and often less constrained, ALP-fermion couplings, as discussed in [24].

In Tab. 2 the decay rates of several neutral meson decays are collected. For definiteness, again $m_a = 0$, $f_a = 1$ TeV and $c_f = \pm 1$ have been used. The same formula discussed for the charged meson decays can be straightforwardly obtained also for the neutral meson case. In particular, penguin amplitudes typically dominate over tree-level ones, when available. The only exception being again represented by the D meson sector, where tree-level amplitudes are at least one order of magnitude larger than penguin ones.

The Kaon sector is the sector from which the most precise bounds on ALP-fermion couplings are obtained [21,24,44], thanks to very precise decay rate measurements. In particular NA62 at CERN, looking at $K^+ \rightarrow \pi^+ a$, has collected 3×10^{16} p.o.t. in Run 1 and is aiming for 10^{18} p.o.t by the end of Run 2. Using the complete Run 1 dataset, the NA62 experiment established an upper limit on the $\mathcal{B}(K^+ \rightarrow \pi^+ a)$ for an invisible ALP at the level of 10^{-11} in the mass ranges of 0–110 MeV and 155–260 MeV [55,56]. NA62 experiment has also established upper limits on $\mathcal{B}(K^+ \rightarrow \pi^+ a) \lesssim 10^{-9}$ in the 110–115 MeV mass range, i.e. around of the π_0 mass, from a dedicated analysis based on the 10% of the Run 1 minimum bias dataset [54]. Measurements of the $K_L^0 \rightarrow \pi^0 \bar{\nu} \nu$ decay naturally provide limits on the $\mathcal{B}(K_L^0 \rightarrow \pi^0 a)$ branching ratio. KOTO experiment [58] has reported a limit on $\mathcal{B}(K_L^0 \rightarrow \pi^0 a) \lesssim 2.4 \times 10^{-9}$ at 90% CL with the 2015 dataset, practically independent on the ALP mass up to the kinematical limit.

In Fig. 7 a summary of the constraints on the quark couplings from K hadronic decays into an invisible ALP are collected as function of the mass m_a and for the chosen reference value $f_a = 1$ TeV. The pink (middle) and red (lower) shaded areas show the bounds directly derived in Ref. [24] from the $K^+ \rightarrow \pi^+ a$ decay rate. The pink area represents the limits projected onto the ALP-valence s- and u-quarks couplings, assuming all the other ALP-fermion coupling vanishing. Given that the tree-level amplitude is largely dominated by the ISR amplitude, it depends mainly on c_s and c_u . The highlighted region has a meaning similar to the range displayed in Tab. 1 and 2, i.e. the boundaries of the region correspond to two the limiting cases $c_u = \pm c_s$. The single parameter limit on $c_{s(u)}$, obtained by setting $c_{u(s)} = 0$, lies approximately in the middle of the allowed range. The red (lower) shaded area, instead, represents the bound on c_t obtained by NA62 data assuming a non vanishing c_t coupling and letting c_s vary in the range $[-0.05, 0.05]$. Therefore, despite the fact that the penguin contribution to the $K^+ \rightarrow \pi^+ a$ decay is two order of magnitude larger than the tree-level one, a contamination of the c_t coupling of roughly one order of magnitude is still possible⁵. The single parameter limit on c_t , obtained by setting all other $c_i = 0$, lies

⁵See Ref. [24] for a detailed discussion on the ALP-fermion couplings bounds from $K \rightarrow \pi a$

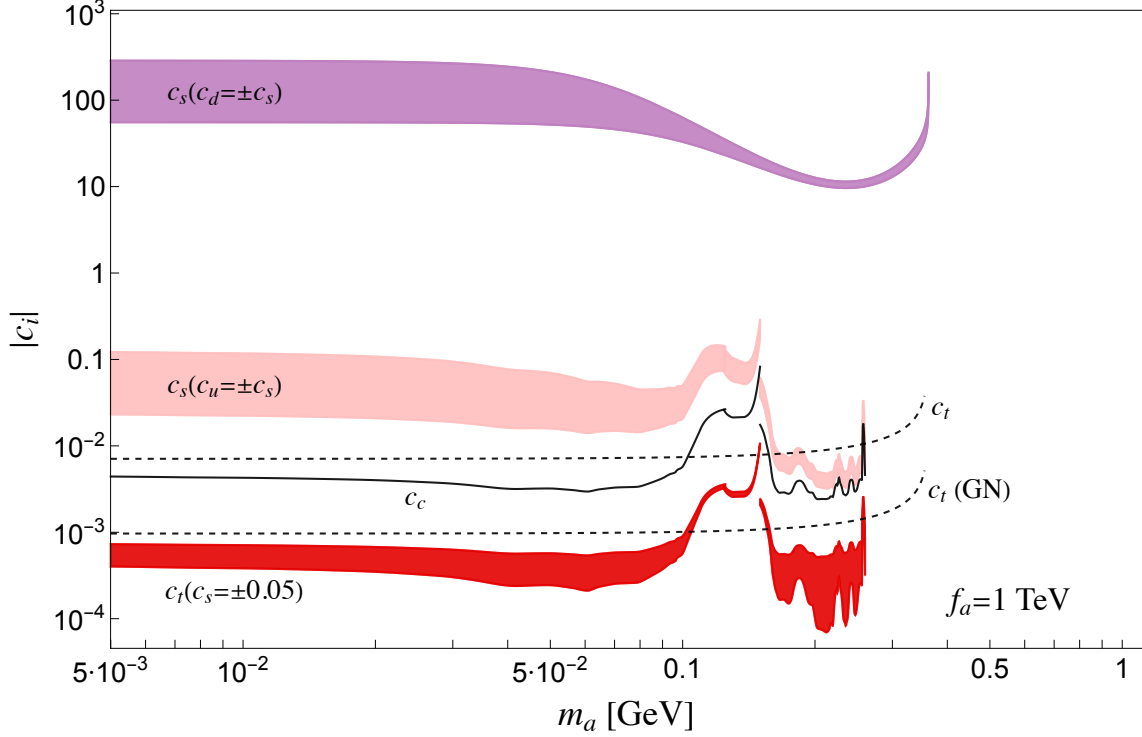


Figure 7: Limits on ALP-quark couplings from hadronic K meson decays, as function of the ALP mass m_a for $f_a = 1$ TeV. The meaning of the different lines/regions is explained in the text.

approximately in the middle of the allowed range. The continuous middle black line shows the single parameter limit on c_c , coupling associated to the sub-dominant term weighting roughly 10% of the total penguin contribution. The upper black dashed line represents the exclusion limit on the c_t parameter, obtained from the KOTO $K_L^0 \rightarrow \pi^0 \nu \bar{\nu}$ measurements, while the lower black dashed one represents the exclusion limit on c_t obtained using NA62 $K^+ \rightarrow \pi^+ \nu \bar{\nu}$ branching ratio for inferring a limit on the K_L^0 branching ratio through the Grossman-Nir bound. As the top penguin loop largely dominates the K_L^0 decay rate, see Tab. 2, no appreciable contamination from the tree-level diagrams is expected. Finally the (upper) violet shaded area represents the limits projected onto the ALP-valence s- and d-quarks couplings from the KOTO K_L^0 measurement, assuming all the other ALP-fermion coupling vanishing and corresponding to the two limiting cases $c_d = \pm c_s$. Therefore, in Fig. 7 an exhaustive set of bounds on ALP-quark couplings obtained from hadronic K decays is collected. The

decays.

single parameter limits obtained from hadronic K decays are also reported in Fig. 8 as continuous colored lines, for comparison.

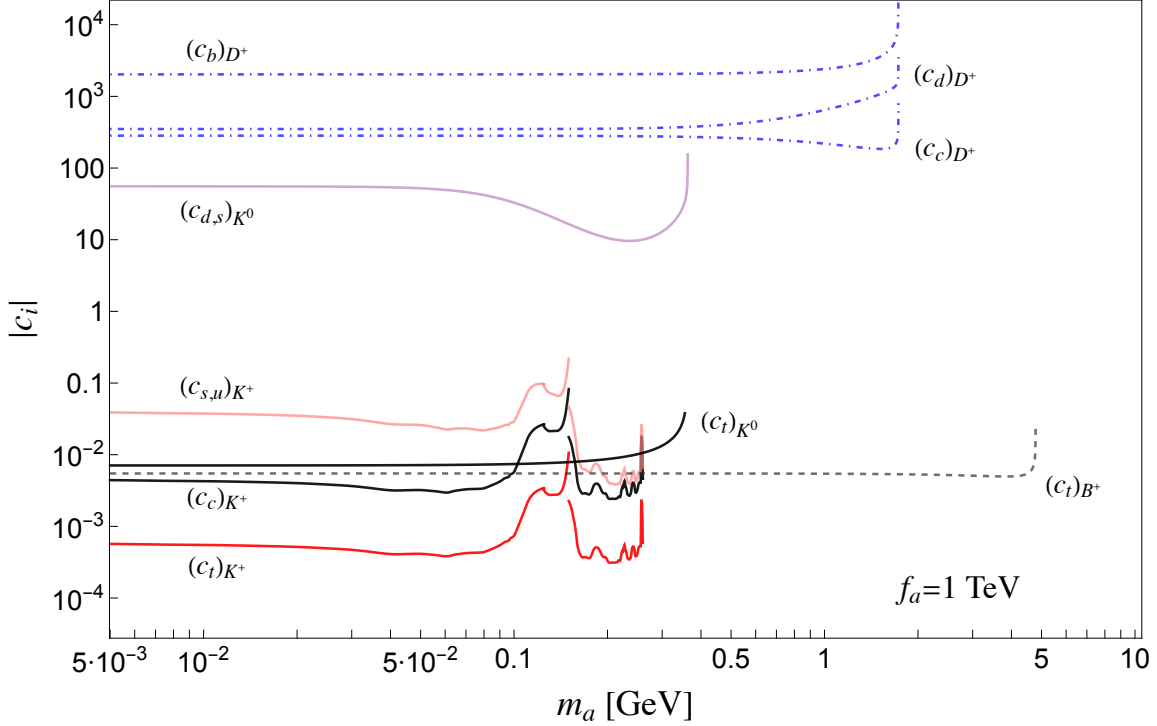


Figure 8: Limits on ALP-quark couplings from hadronic meson decays, as function of the ALP mass m_a for $f_a = 1$ TeV. The meaning of the different lines is explained in the text.

Hadronic B meson decays in ALP are expected to provide additional interesting bounds on ALP-fermion couplings. Still not competing with the ones extracted from K decays, these bounds nevertheless suffer from a smaller theoretical uncertainty and extend the m_a range of constraints up to a few GeV. The first thing one can notice from Tab. 1 and Tab. 2 is that, for the B meson sector, the tree-level vs loop ratio is two/three order smaller compared to the K meson ratio, mainly due to the larger CKM suppression factor. Therefore, one expects practically no contamination on the c_t bounds from ALP-fermion couplings entering in the tree-level amplitudes, assuming perturbativity. The lower dashed black line in Fig. 8 is the c_t exclusion bounds obtained from the recent $B \rightarrow Ka$ Belle II data [66]. Limits on B valence quark couplings are extremely weak due to the smallness of the tree-level amplitude

and lie in the $(10^4 - 10^5)$ region and are not shown in figure⁶. From Tab. 1 one can identify another very promising channel, namely $B_c^+ \rightarrow D_s^+ a$. A future experimental limit on $\text{Br}(B_c^+ \rightarrow D_s^+ a) < 10^{-5}$ would provide competitive bounds on c_t . Other theoretically interesting channels are hadronic B_c decays into vector meson, like $B_c^\pm \rightarrow \rho(K^*) a$. These decays have no penguin contribution and a small $M_{\rho, K^*}/M_{B_c}$ mass ratio. Therefore a very clean extraction on ALP- B_c valence quark coupling could be addressed.

A complementary set of information can be potentially extracted from hadronic D decays in ALP. Indeed, D -mesons penguins do not dominate anymore over tree-level amplitudes being m_b/m_t suppressed compared to similar B and K meson decays, as shown numerically by Tab. 1 and Tab. 2. At present there are no experimental results measuring hadronic D decays in ALPs, the only information originate from a recast of the charged $D \rightarrow \tau(\rightarrow \pi\nu)\bar{\nu}$ decay onto the $D^\pm \rightarrow \pi^\pm a$ branching ratio, as proposed by Ref. [23]. Even though the predicted signals are quite weak these channels can provide sensitivity on the D^\pm valence quark couplings, c_d and c_c and eventually on c_b through the dominant down-type penguin loop. The individual limits on these ALP-quark couplings, shown in Fig. 8 as dot-dashed lines, appear evidently above the perturbativity region once $f_a = 1$ TeV is chosen.

The single parameter limits obtained from hadronic K meson decays are represented as continuous colored lines. Finally, no experimental data are at present available for K^* and ρ hadronic decays in ALP. The expected pattern is assumed to be, however, very similar to the K s one.

4.2 Leptonic Final States

Pseudoscalar leptonic decay can be used to constraint flavor-diagonal ALP-fermion couplings through the tree-level amplitudes of Eqs. (33) and (36). In the case of invisible ALP, considered throughout this paper, the simplest approach is to saturate the $1\text{-}\sigma$ experimental limits on the corresponding SM leptonic branching ratio adding the pseudoscalar meson three-body leptonic ALP decay to the two-body leptonic SM one, having the same missing energy signature. At present, in fact, there is not enough available experimental information on the charged lepton energy distribution such that one can obtain stricter bounds by characterizing two-body vs three-body decay spectrum⁷.

Leptonic B decays have been measured at Babar and Belle. The latest Belle data for electron, muon and tau channel can be found in [103–105], respectively. Charmed meson decays have been measured at BESS (see [106–108] for D and [109, 110] for D_s

⁶Tree level contributions of B meson valence quark may have possible interferences with initial/final state emission, as commented in Sec. 3.3.

⁷See [25] for more details on three-body spectral analysis of meson leptonic decays in ALP.

Channel	c_i u-type	c_i d-type	c_i leptons
$B^\pm \rightarrow e^\pm \bar{\nu}_e$	360	250	$2 \cdot 10^6$
$B^\pm \rightarrow \mu^\pm \bar{\nu}_\mu$	170	120	$5 \cdot 10^3$
$B^\pm \rightarrow \tau^\pm \bar{\nu}_\tau$	$2.6 \cdot 10^3$	$2 \cdot 10^3$	$5 \cdot 10^3$
$D^\pm \rightarrow e^\pm \bar{\nu}_e$	170	175	$5 \cdot 10^4$
$D^\pm \rightarrow \mu^\pm \bar{\nu}_\mu$	250	270	$3.5 \cdot 10^3$
$D^\pm \rightarrow \tau^\pm \bar{\nu}_\tau$	$1.5 \cdot 10^5$	$1.5 \cdot 10^5$	$1.7 \cdot 10^5$
$D_s^\pm \rightarrow e^\pm \bar{\nu}_e$	125	120	$5 \cdot 10^5$
$D_s^\pm \rightarrow \mu^\pm \bar{\nu}_\mu$	180	175	$3.5 \cdot 10^3$
$D_s^\pm \rightarrow \tau^\pm \bar{\nu}_\tau$	$5 \cdot 10^4$	$1 \cdot 10^5$	$5 \cdot 10^4$
$K^\pm \rightarrow e^\pm \bar{\nu}_e$	4	6	$4 \cdot 10^3$
$K^\pm \rightarrow \mu^\pm \bar{\nu}_\mu$	600	800	$3 \cdot 10^3$

Table 3: Limits on single ALP-fermion coupling c_i derived from pseudoscalar meson leptonic decays for $m_a = 0$ and $f_a = 1$ TeV.

decays respectively) and at Belle [111]. Leptonic Kaon decays have been measured by KLOE and NA62 [69, 112, 113].

The derived bounds on single ALP-fermion couplings, c_i , for $m_a = 0$ and $f_a = 1$ TeV are shown in Tab. 3. As an example, the first row in Tab. 3 should be read as follows: the “up-quark” column represents the limit on c_u by setting $c_b = c_e = 0$, the “down-quark” column represents the limit on c_b by setting $c_u = c_e = 0$, and finally the value in the “lepton” column is the limit on c_e for $c_u = c_b = 0$. It is true in general that hadronic meson decays in ALP can provide by far the most stringent limits on a universal ALP-fermion coupling, bounding $c_{a\Phi} \lesssim 5 \times 10^{-4}$ from K decays or $c_{a\Phi} \lesssim 8 \times 10^{-3}$ from B decays, for $f_a = 1$ TeV. However, both these limits come associated to the top enhanced penguin, and therefore in a non-universal ALP-fermion coupling scenario can be applied to bound solely c_t . On the contrary, leptonic and hadronic decays in ALP often provide similar constrains on single ALP-light-quark couplings, as can be seen comparing the results of Tab. 3 with the ones summarized in Fig. 8. While, for example, single parameter bounds on $c_{u,s}$ derived from charged K hadronic decay are still one order of magnitude better than the ones obtained from charged K leptonic channel, conversely c_c bounds obtained from charged D meson leptonic decay are of the same order, or even slightly better than the corresponding charged D meson hadronic ones. Finally, c_b bounds from charged B meson leptonic decays are at least two order of magnitude better than the hadronic limits. Therefore, meson leptonic decays provide useful complementary information once independent bounds on all the ALP-quark couplings are needed.

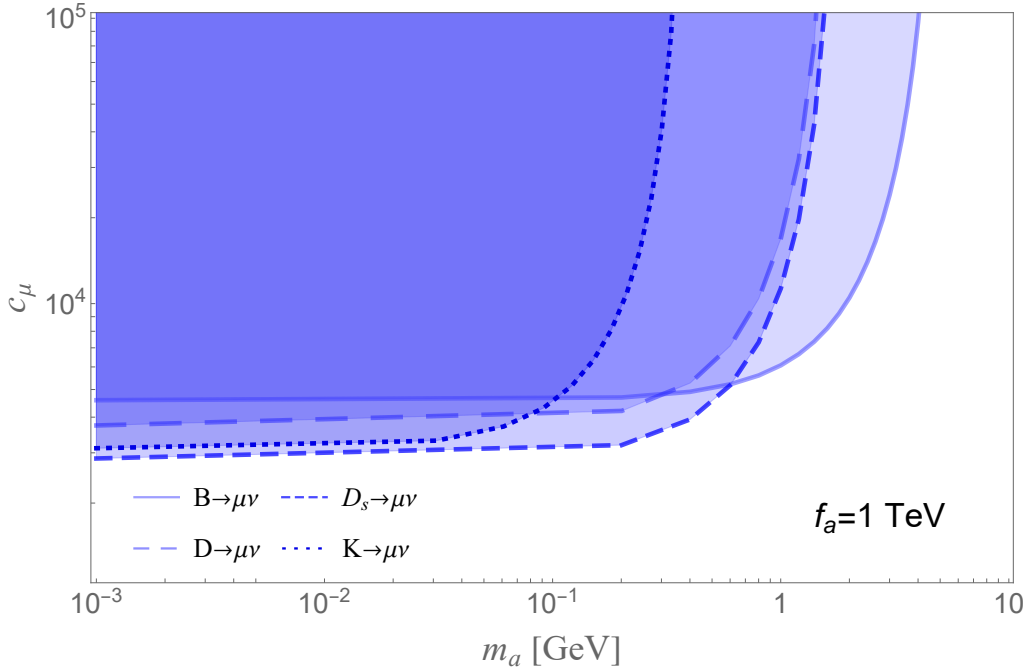


Figure 9: Summary of the limits extracted from the semileptonic class, $M \rightarrow \ell\nu a$, on the muonic coupling c_μ with f_a fixed at 1 TeV.

From Tab. 3, evidently emerges that limits on ALP-lepton coupling are very weak, due to the combination of low masses (i.e. the electron case) and/or not very precise experimental results (i.e. the τ channels). However, despite these feeble bounds, pseudoscalar meson leptonic decays in ALP provide undoubtedly the best available limits on the ALP-lepton sector for an m_a in the KeV-GeV range. In Fig. 9, for exemplification, all the limits on the muon coupling, c_μ , are collected as function of the ALP mass m_a , for the chosen values $f_a = 1$ TeV. From the plot one can easily discern a slower saturation of the kinematical limit compared to the corresponding hadronic decays. Already at values $m_a \approx M_M/2$ a strong reduction of the decay rate appears. One can easily understand from the corresponding Dalitz plot that this effect is associated to the tree-body nature of the leptonic meson decay in ALP. Therefore some additional caution should be used in this case to generalize the validity of $m_a = 0$ results to higher mass values.

4.3 Phenomenological Summary

Finally, a comprehensive summary of all the bounds on flavor conserving ALP-fermion couplings derived in the previous section is presented in Fig. 10. To be able

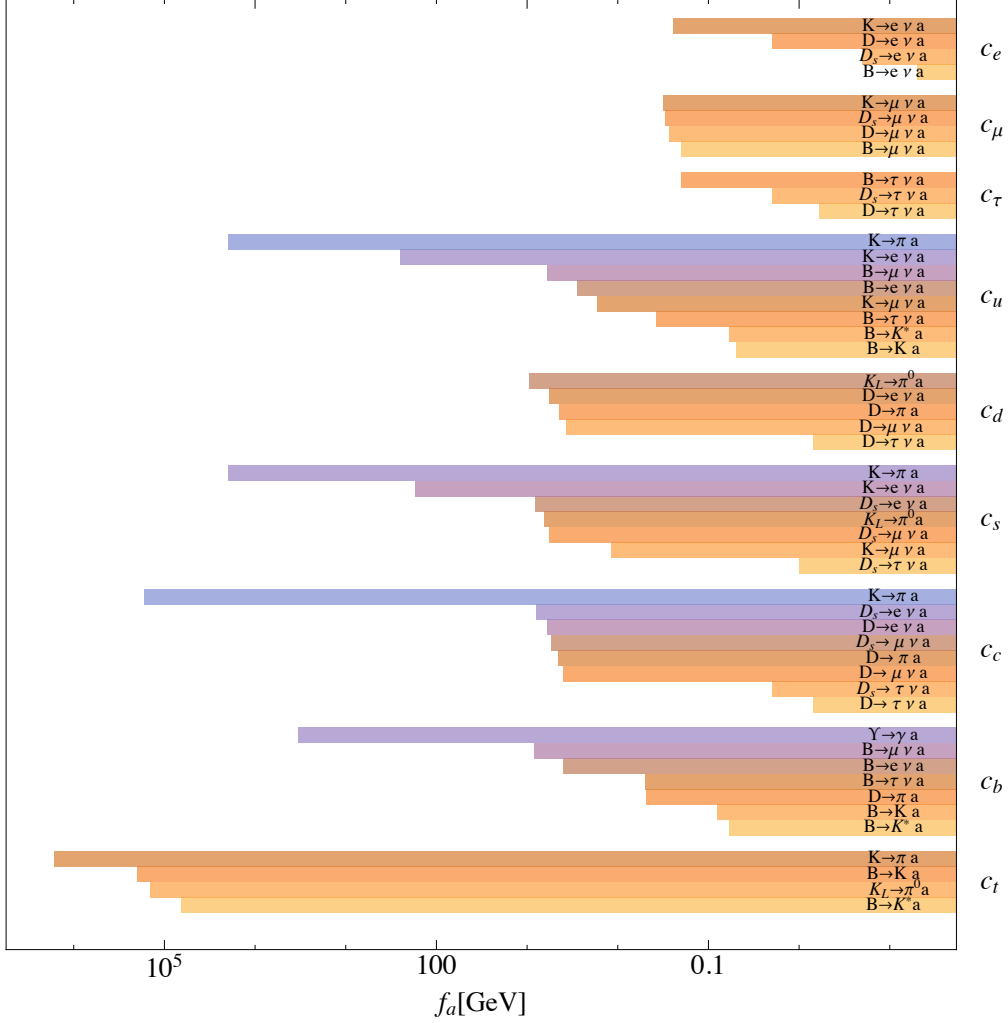


Figure 10: Bounds on f_a (expressed in GeV) obtained from meson decays into an invisible ALP, for $m_a = 0$ and assuming the corresponding $c_i = 1$, while setting all the other couplings to 0.

to fairly compare all the different analysis, the limits on the $U(1)_{PQ}$ breaking scale f_a (expressed in GeV) are shown, for $m_a = 0$ and by assuming the corresponding $c_i = 1$, with all the other couplings set to 0. Therefore, the f_a value plotted represents the highest energy scale tested, at present, in each decay channel. One can notice that the most stringent bounds on f_a come from the top sector, trough the m_t enhanced penguin contributions [21, 24]. From K and B hadronic pseudoscalar meson decays one tests $f_a \simeq (10^5 - 10^6)$ GeV. This is the lowest energy scale at which new physics in the ALP sector may appear, when a universal ALP-fermion coupling is assumed.

$K \rightarrow \pi a$ decay provides the strongest bounds for all the ALP-quark couplings in the non-universal, but flavor conserving ALP-fermion scenario, with the only exception of the ALP-bottom coupling where the strongest bound comes from the $\Upsilon(ns) \rightarrow \gamma a$ decay [22]. Bounds on $c_{t,c}$ enter from the penguin loop diagram, while bounds on $c_{u,d,s}$ are due to the tree-level amplitude contribution. Meson leptonic decays produces an upper bound on $f_a \simeq (10^{-1} - 10)$ GeV in the ALP-lepton sector.

5 Conclusions

In this paper, bounds on non-universal flavor-diagonal ALP-fermion couplings are presented. These limits have been extracted from mesonic decays assuming an invisible ALP signature. Two large classes of processes are studied: i) hadronic meson decays $M_I \rightarrow M_F a$, with M_I and M_F pseudoscalar and/or vector mesons and ii) leptonic meson decays $M \rightarrow \ell \nu a$. Lattice QCD and Brodsky-Lepage method are used for calculating the hadronic matrix elements associated to local and bi-local operators respectively. In particular, a complete set of tree-level amplitudes intervening in mesonic ALP decays have been derived for the first time, allowing a general comparison between tree-level and penguin mediated processes. For example, hadronic K and B decays in ALP are both clearly top-penguin dominated. However, already from a quick analysis of Eq. (55) one can estimate the different level of parameter cross-contamination that one could expect in a general non universal flavor conserving framework: while can be sizable for the case of K meson hadronic decays, as exemplified in Fig. 7, it is instead completely negligible for the B sector as explained in the text and shown in Fig. 10. Conversely, hadronic D meson decays are typically tree-level dominated but a large penguin contamination is however expected. Moreover, a complete analysis of the independent limits on the different ALP-charged lepton diagonal couplings has been presented. Despite being several order of magnitude less constrained than the quark counterpart, these bounds extend previous limits, obtained mainly from astrophysical data, to the KeV-GeV ALP mass range. Finally, for completeness in App. A a recast of the bounds in term of general, non-diagonal, ALP-fermion couplings is presented.

The work presented here can be easily extended to visible ALP decays. It is however phenomenologically much more complicated to use those data for performing model independent analysis, as each decay amplitude will depend on the combinations of products of two different ALP-fermion couplings.

6 Acknowledgements

We thank Xavier Ponce Díaz for useful discussion. A.G. and S.R. acknowledge support from the European Union's Horizon 2020 research and innovation programme under the Marie Skłodowska-Curie grant agreements 690575 (RISE InvisiblesPlus), 674896 (ITN ELUSIVES) and 860881 (HIDDEN).

A Limits on Flavor Violating Couplings

For the sake of completeness a projection of the limits induced onto the flavor changing parameters of the Lagrangian in Eq. (1), is presented here. The dimension five ALP-quark Lagrangian reads:

$$\mathcal{L}_{\text{FC}}^a = \frac{\partial_\mu a}{2f_a} \bar{d} \gamma^\mu (C_V^{(d)} + C_A^{(d)} \gamma^5) d + \frac{\partial_\mu a}{2f_a} \bar{u} \gamma^\mu (C_V^{(u)} + C_A^{(u)} \gamma^5) u. \quad (56)$$

V -type couplings will induce parity conserving mesonic decays such as $\mathcal{P}_I \rightarrow \mathcal{P}_F a$ and $\mathcal{V}_I \rightarrow \mathcal{V}_F a$, while A -type one will enter in parity violating processes such as $\mathcal{P} \rightarrow \mathcal{V} a$.

Two different scenarios may be considered: 1) flavor violation is induced by tree level parameters or 2) flavor violation is induced by effective couplings that emerge due to RG effects. In the first scenario, the $M_I \rightarrow M_F a$ branching ratio, in the ALP massless limit, reads:

$$\text{Br}(M_I \rightarrow M_F a) = \kappa \frac{M_I^3}{16\pi\Gamma_I} \frac{\left| (C_{A,V}^{(u,d)})_{ij} \right|^2}{4f_a^2} F(m_a^2)^2 \left(1 - \frac{M_F^2}{M_I^2} \right)^3, \quad (57)$$

where $(C_{A,V}^{(q)})_{ij}$ is the relevant coupling mediating the FC transition and $F(m_a^2)$ is the associated hadronic form factor. The parameter κ is 1 (1/3) if M_I is a pseudoscalar (vector) meson respectively. The bounds extracted from hadronic meson decays into an invisible ALP are collected in Tab. 4, for the chosen value $f_a = 1$ TeV. From $K^+ \rightarrow \pi^+ a$ decay one can test the sd -vector sector, $(C_V^{(d)})_{sd}$. To bound the sd -axial sector, $(C_A^{(d)})_{sd}$, one could use the $K^* \rightarrow \pi a$ decays. These decays, however, are not measured yet, and therefore such limits have to be expressed as function of a still unknown branching ratio (Br):

$$\left| (C_A^{(d)})_{sd} \right| = 6 \cdot 10^3 \cdot [\text{Br}(K^* \rightarrow \pi a)]^{1/2} \text{ GeV}^{-1}. \quad (58)$$

The $B^+ \rightarrow K^+ a$ and $B^+ \rightarrow K^{*+} a$ channels provide exclusion limits on $(C_V^{(d)})_{bs}$ and $(C_A^{(d)})_{bs}$ respectively. Finally $(C_V^{(d)})_{bd}$ and $(C_A^{(d)})_{bd}$ can be tested via $B \rightarrow \pi(\rho) a$ decays.

Again, as the $B \rightarrow \rho \cancel{E}$ branching ratio is not measured one can express the bound as

$$\left| (C_A^{(d)})_{bd} \right| = 7.4 \cdot 10^{-4} \cdot [\text{Br}(B \rightarrow \rho a)]^{1/2} \text{ GeV}^{-1}. \quad (59)$$

The numerical difference between Eq. (58) and (59) is due to the huge difference in the mean life of the resonances. In the up-quark sector only the cu sector can be tested via $D^+ \rightarrow \pi^+(\rho^+)a$, yet not measured. Therefore, the limit on $(C_A^{(u)})_{cu}$ is once again expressed as:

$$\left| (C_A^{(u)})_{cu} \right| = 4.5 \cdot 10^{-3} \cdot [\text{Br}(D \rightarrow \rho a)]^{1/2} \text{ GeV}^{-1}. \quad (60)$$

However, a limit on $(C_V^{(u)})_{cu}$ can be extracted following Ref. [23] and using a recast of $D^+ \rightarrow \tau^+(\rightarrow \pi^+\nu)\bar{\nu}$ giving $\text{Br}(D^+ \rightarrow \pi^+a) < 8 \cdot 10^{-6}$. Processes involving top quark transitions are clearly not yet accessible.

Vector	Limit	Axial	Limit
$ (C_V^{(d)})_{sd} /f_a$	$2.5 \cdot 10^{-12} \text{ GeV}^{-1}$	$ (C_A^{(d)})_{sd} /f_a$	n.a.
$ (C_V^{(d)})_{bs} /f_a$	$9 \cdot 10^{-9} \text{ GeV}^{-1}$	$ (C_A^{(d)})_{bs} /f_a$	$1.3 \cdot 10^{-8} \text{ GeV}^{-1}$
$ (C_V^{(d)})_{bd} /f_a$	$1 \cdot 10^{-8} \text{ GeV}^{-1}$	$ (C_A^{(d)})_{bd} /f_a$	n.a.
$ (C_V^{(u)})_{cu} /f_a$	$2 \cdot 10^{-8} \text{ GeV}^{-1}$	$ (C_A^{(u)})_{cu} /f_a$	n.a.

Table 4: Limits on flavor violating couplings in the scenario 1) for $m_a = 0$ and $f_a = 1$ TeV.

In the second considered scenario one can set to 0 the off-diagonal parameters of Eq. (56) at the high scale f_a . This procedure does not get rid completely of flavor-violation in the ALP-sector, as it can be generated from the flavor conserving parameters via RG equations proportionally the SM flavor violation induced by the CMK matrix [26]. One can project limits on these effective couplings by equating the amplitude of a given process obtained from Eq. (56) to the amplitudes in Eq. (50) and (53) for V/A type couplings respectively. The off-diagonal entries of the matrices are to be considered not as tree level parameters, but as effective ones, induced by diagonal couplings. In principle there are four different matrices in the Lagrangian in Eq. (56), but this scenario does not distinguishes axial or vector off-diagonal elements. The effective flavor violating couplings read:

$$C_{ij}^{(d/u)} = \frac{G_F m_q^2}{2\sqrt{2}\pi^2} \sum_f c_{ij}^{(f)} = \frac{G_F m_q^2}{2\sqrt{2}\pi^2} \sum_f V_{fi} V_{fj}^* c_f \frac{x_f}{x_q} \ln \left(\frac{f_a^2}{m_f^2} \right) \quad (61)$$

where the sum over the f runs on up-type quarks for $C^{(d)}$ and on down-type quarks for $C^{(u)}$, and m_q is the mass of the heaviest quark running in the loop. The limits

shown in Fig. 10, recasted onto bounds on $C^{(d/u)}$, are reported in Tab. 5, for $f_a = 1$ TeV.

d -type	Limit	u -type	Limit
$ (C^{(d)})_{sd} /f_a$	$3.8 \cdot 10^{-12} \text{ GeV}^{-1}$	$ (C^{(u)})_{cu} /f_a$	$3.2 \cdot 10^{-12} \text{ GeV}^{-1}$
$ (C^{(d)})_{bs} /f_a$	$4.3 \cdot 10^{-10} \text{ GeV}^{-1}$	$ (C^{(u)})_{tc} /f_a$	$9.1 \cdot 10^{-10} \text{ GeV}^{-1}$
$ (C^{(d)})_{bd} /f_a$	$9.3 \cdot 10^{-11} \text{ GeV}^{-1}$	$ (C^{(u)})_{tu} /f_a$	$7.7 \cdot 10^{-11} \text{ GeV}^{-1}$

Table 5: Limits on flavor violating couplings in the scenario 2) for $m_a = 0$ and $f_a = 1$ TeV.

References

- [1] R.D. Peccei and Helen R. Quinn. CP Conservation in the Presence of Instantons. *Phys. Rev. Lett.*, 38:1440–1443, 1977.
- [2] R. D. Peccei and Helen R. Quinn. Constraints imposed by CP conservation in the presence of pseudoparticles. *Phys. Rev. D*, 16:1791–1797, Sep 1977.
- [3] F. Wilczek. Problem of strong p and t invariance in the presence of instantons. *Phys. Rev. Lett.*, 40:279–282, Jan 1978.
- [4] Steven Weinberg. A new light boson? *Phys. Rev. Lett.*, 40:223–226, Jan 1978.
- [5] Varouzhan Baluni. CP-nonconserving effects in quantum chromodynamics. *Phys. Rev. D*, 19:2227–2230, Apr 1979.
- [6] R.J. Crewther, P. Di Vecchia, G. Veneziano, and E. Witten. Chiral estimate of the electric dipole moment of the neutron in quantum chromodynamics. *Physics Letters B*, 88(1):123–127, 1979.
- [7] Maxim Pospelov and Adam Ritz. Electric dipole moments as probes of new physics. *Annals Phys.*, 318:119–169, 2005, [arXiv: hep-ph/0504231](https://arxiv.org/abs/hep-ph/0504231).
- [8] Jihn E. Kim and Gianpaolo Carosi. Axions and the strong cp problem. *Rev. Mod. Phys.*, 82:557–601, Mar 2010.
- [9] C. A. Baker, D. D. Doyle, P. Geltenbort, K. Green, M. G. D. van der Grinten, P. G. Harris, P. Iaydjiev, S. N. Ivanov, D. J. R. May, J. M. Pendlebury, J. D. Richardson, D. Shiers, and K. F. Smith. Improved experimental limit on the electric dipole moment of the neutron. *Phys. Rev. Lett.*, 97:131801, Sep 2006.

- [10] Michele Cicoli. Axion-like Particles from String Compactifications. In *9th Patras Workshop on Axions, WIMPs and WISPs*, pages 235–242, 2013, [arXiv: 1309.6988 \[hep-th\]](#).
- [11] Frank Wilczek. Axions and family symmetry breaking. *Phys. Rev. Lett.*, 49:1549–1552, Nov 1982.
- [12] Jonathan L. Feng, Takeo Moroi, Hitoshi Murayama, and Erhard Schnapka. Third generation familons, b factories, and neutrino cosmology. *Phys. Rev. D*, 57:5875–5892, 1998, [arXiv: hep-ph/9709411](#).
- [13] Lorenzo Calibbi, Florian Goertz, Diego Redigolo, Robert Ziegler, and Jure Zupan. Minimal axion model from flavor. *Phys. Rev. D*, 95(9):095009, 2017, [arXiv: 1612.08040 \[hep-ph\]](#).
- [14] Yohei Ema, Koichi Hamaguchi, Takeo Moroi, and Kazunori Nakayama. Flaxion: a minimal extension to solve puzzles in the standard model. *JHEP*, 01:096, 2017, [arXiv: 1612.05492 \[hep-ph\]](#).
- [15] Peter W. Graham, David E. Kaplan, and Surjeet Rajendran. Cosmological Relaxation of the Electroweak Scale. *Phys. Rev. Lett.*, 115(22):221801, 2015, [arXiv: 1504.07551 \[hep-ph\]](#).
- [16] John Preskill, Mark B. Wise, and Frank Wilczek. Cosmology of the Invisible Axion. *Phys. Lett. B*, 120:127–132, 1983.
- [17] L. F. Abbott and P. Sikivie. A Cosmological Bound on the Invisible Axion. *Phys. Lett. B*, 120:133–136, 1983.
- [18] Michael Dine and Willy Fischler. The Not So Harmless Axion. *Phys. Lett. B*, 120:137–141, 1983.
- [19] Howard Georgi, David B. Kaplan, and Lisa Randall. Manifesting the Invisible Axion at Low-energies. *Phys. Lett. B*, 169:73–78, 1986.
- [20] Y.G. Aditya, Kristopher J. Healey, and Alexey A. Petrov. Searching for super-WIMPs in leptonic heavy meson decays. *Phys. Lett. B*, 710:118–124, 2012, [arXiv: 1201.1007 \[hep-ph\]](#).
- [21] M.B. Gavela, R. Houtz, P. Quilez, R. Del Rey, and O. Sumensari. Flavor constraints on electroweak ALP couplings. *Eur. Phys. J. C*, 79(5):369, 2019, [arXiv: 1901.02031 \[hep-ph\]](#).

- [22] L. Merlo, F. Pobbe, S. Rigolin, and O. Sumensari. Revisiting the production of ALPs at B-factories. *JHEP*, 06:091, 2019, [arXiv: 1905.03259 \[hep-ph\]](#).
- [23] Jorge Martin Camalich, Maxim Pospelov, Pham Ngoc Hoa Vuong, Robert Ziegler, and Jure Zupan. Quark Flavor Phenomenology of the QCD Axion. *Phys. Rev. D*, 102(1):015023, 2020, [arXiv: 2002.04623 \[hep-ph\]](#).
- [24] Alfredo Walter Mario Guerrero and Stefano Rigolin. Revisiting $K \rightarrow \pi a$ decays. *Eur. Phys. J. C*, 82(3):192, 2022, [arXiv: 2106.05910 \[hep-ph\]](#).
- [25] Jorge Alda Gallo, Alfredo Walter Mario Guerrero, Siannah Peñaranda, and Stefano Rigolin. Leptonic meson decays into invisible ALP. *Nucl. Phys. B*, 979:115791, 2022, [arXiv: 2111.02536 \[hep-ph\]](#).
- [26] Martin Bauer, Matthias Neubert, Sophie Renner, Marvin Schnubel, and Andrea Thamm. The Low-Energy Effective Theory of Axions and ALPs. *JHEP*, 04:063, 2021, [arXiv: 2012.12272 \[hep-ph\]](#).
- [27] G. D’Ambrosio, G. F. Giudice, G. Isidori, and A. Strumia. Minimal flavor violation: An Effective field theory approach. *Nucl. Phys. B*, 645:155–187, 2002, [arXiv: hep-ph/0207036](#).
- [28] P. Sikivie. Experimental tests of the ”invisible” axion. *Phys. Rev. Lett.*, 51:1415–1417, Oct 1983.
- [29] K. Zioutas et al. A Decommissioned LHC model magnet as an axion telescope. *Nucl. Instrum. Meth. A*, 425:480–489, 1999, [arXiv: astro-ph/9801176](#).
- [30] I.G Irastorza, F.T Avignone, S Caspi, J.M Carmona, T Dafni, M Davenport, A Dudarev, G Fanourakis, E Ferrer-Ribas, J Galán, J.A García, T Gerasis, I Giomataris, H Gómez, D.H.H Hoffmann, F.J Iguaz, K Jakovčić, M Krčmar, B Lakić, G Luzón, M Pivovarov, T Papaevangelou, G Raffelt, J Redondo, A Rodríguez, S Russenschuck, J Ruz, I Shilon, H. Ten Kate, A Tomás, S Troitsky, K. van Bibber, J.A Villar, J Vogel, L Walckiers, and K Zioutas. Towards a new generation axion helioscope. *Journal of Cosmology and Astroparticle Physics*, 2011(06):013–013, jun 2011.
- [31] Igor G Irastorza, E. Armengaud, F. T. Avignone, M. Betz, P. Brax, P. Brun, G. Cantatore, J. M. Carmona, G. P. Carosi, F. Caspers, S. Caspi, S. A. Cetin, D. Chelouche, F. E. Christensen, A. Dael, T. Dafni, M. Davenport, A.V. Derbin, K. Desch, A. Diago, B. D. Dobrich, I. Dratchnev, A. Dudarev, C. Eleftheriadis, G. Fanourakis, E. Ferrer-Ribas, J. Galan, J. A. Garcia, J. G. Garza, T. Gerasis, B. Gimeno, I. Giomataris, S. Gninenko, H. Gomez, D. Gonzalez-Diaz,

- E. Guendelman, C. J. Hailey, T. Hiramatsu, D. H. H. Hoffmann, D. Horns, F. J. Iguaz, J. Isern, K. Imai, A. C. Jakobsen, J. Jaeckel, K. Jakovcic, J. Kaminski, M. Kawasaki, M. Karuza, M. Krcmar, K. Kousouris, C. Krieger, B. Lakic, O. Limousin, A. Lindner, A. Liolios, G. Luzon, S. Matsuki, V. N. Muratova, C. Nones, I. Ortega, T. Papaevangelou, M. J. Pivovarov, G. Raffelt, J. Redondo, A. Ringwald, S. Russenschuck, J. Ruz, K. Saikawa, I. Savvidis, T. Sekiguchi, Y. K. Semertzidis, I. Shilon, P. Sikivie, H. Silva, H. ten Kate, A. Tomas, S. Troitsky, T. Vafeiadis, K. van Bibber, P. Vadrine, J. A. Villar, J. K. Vogel, L. Walkiers, A. Weltman, W. Wester, S. C. Yildiz, and K. Zioutas. The International Axion Observatory IAXO. Letter of Intent to the CERN SPS committee. Technical Report CERN-SPSC-2013-022. SPSC-I-242, CERN, Geneva, Aug 2013.
- [32] Yonatan Kahn, Benjamin R. Safdi, and Jesse Thaler. Broadband and resonant approaches to axion dark matter detection. *Phys. Rev. Lett.*, 117:141801, Sep 2016.
- [33] Jonathan L. Ouellet, Chiara P. Salemi, Joshua W. Foster, Reyco Henning, Zachary Bogorad, Janet M. Conrad, Joseph A. Formaggio, Yonatan Kahn, Joe Minervini, Alexey Radovinsky, Nicholas L. Rodd, Benjamin R. Safdi, Jesse Thaler, Daniel Winklehner, and Lindley Winslow. First results from abracadabra-10 cm: A search for sub- μeV axion dark matter. *Phys. Rev. Lett.*, 122:121802, Mar 2019.
- [34] Allen Caldwell, Gia Dvali, Béla Majorovits, Alexander Millar, Georg Raffelt, Javier Redondo, Olaf Reimann, Frank Simon, and Frank Steffen. Dielectric haloscopes: A new way to detect axion dark matter. *Phys. Rev. Lett.*, 118:091801, Mar 2017.
- [35] Yannis K. Semertzidis et al. Axion Dark Matter Research with IBS/CAPP. 10 2019, [arXiv: 1910.11591](https://arxiv.org/abs/1910.11591) [physics.ins-det].
- [36] Adrian Ayala, Inma Domínguez, Maurizio Giannotti, Alessandro Mirizzi, and Oscar Straniero. Revisiting the bound on axion-photon coupling from Globular Clusters. *Phys. Rev. Lett.*, 113(19):191302, 2014, [arXiv: 1406.6053](https://arxiv.org/abs/1406.6053) [astro-ph.SR].
- [37] Oscar Straniero, Adrian Ayala, Maurizio Giannotti, Alessandro Mirizzi, and Inma Dominguez. Axion-Photon Coupling: Astrophysical Constraints. In *Straniero, Oscar "Axion-Photon Coupling: Astrophysical Constraints" in Proceedings, 11th Patras Workshop on Axions, WIMPs and WISPs (Axion-WIMP 2015) / Irastorza, Igor G., Redondo, Javier, Carmona, Jose Manuel, Cebrian, Susana, Dafni, Theopisti, Iguaz, Francisco J., Luzon, Gloria (eds.), Verlag*

Deutsches Elektronen-Synchrotron : 2015 ; AXION-WIMP 2015 : 11th Patras Workshop on Axions, WIMPs and WISPs, 2015-06-22 - 2015-06-26, Zaragoza, DESY-PROC, pages 77–81, Hamburg, Jun 2015. 11th Patras Workshop on Axions, WIMPs and WISPs, Zaragoza (Spain), 22 Jun 2015 - 26 Jun 2015, Verlag Deutsches Elektronen-Synchrotron.

- [38] N. Vinyoles, A. Serenelli, F.L. Villante, S. Basu, J. Redondo, and J. Isern. New axion and hidden photon constraints from a solar data global fit. *Journal of Cosmology and Astroparticle Physics*, 2015(10):015–015, oct 2015.
- [39] E. Aprile et al. First Axion Results from the XENON100 Experiment. *Phys. Rev. D*, 90(6):062009, 2014, [arXiv: 1404.1455 \[astro-ph.CO\]](https://arxiv.org/abs/1404.1455). [Erratum: *Phys.Rev.D* 95, 029904 (2017)].
- [40] D. S. Akerib, S. Alsum, C. Aquino, H. M. Araújo, X. Bai, A. J. Bailey, J. Balajthy, P. Beltrame, E. P. Bernard, A. Bernstein, T. P. Biesiadzinski, E. M. Boulton, P. Brás, D. Byram, S. B. Cahn, M. C. Carmona-Benitez, C. Chan, A. A. Chiller, C. Chiller, A. Currie, J. E. Cutter, T. J. R. Davison, A. Dobi, J. E. Y. Dobson, E. Druskiewicz, B. N. Edwards, C. H. Faham, S. R. Fallon, S. Fiorucci, R. J. Gaitskell, V. M. Gehman, C. Ghag, K. R. Gibson, M. G. D. Gilchriese, C. R. Hall, M. Hanhardt, S. J. Haselschwardt, S. A. Hertel, D. P. Hogan, M. Horn, D. Q. Huang, C. M. Ignarra, R. G. Jacobsen, W. Ji, K. Kamdin, K. Kazkaz, D. Khaitan, R. Knoche, N. A. Larsen, C. Lee, B. G. Lenardo, K. T. Lesko, A. Lindote, M. I. Lopes, A. Manalaysay, R. L. Mannino, M. F. Marzioni, D. N. McKinsey, D.-M. Mei, J. Mock, M. Moongweluwan, J. A. Morad, A. St. J. Murphy, C. Nehr Korn, H. N. Nelson, F. Neves, K. O’Sullivan, K. C. Oliver-Mallory, K. J. Palladino, E. K. Pease, L. Reichhart, C. Rhyne, S. Shaw, T. A. Shutt, C. Silva, M. Solmaz, V. N. Solovov, P. Sorensen, S. Stephenson, T. J. Sumner, M. Szydakis, D. J. Taylor, W. C. Taylor, B. P. Tennyson, P. A. Terman, D. R. Tiedt, W. H. To, M. Tripathi, L. Tvrznikova, S. Uvarov, V. Velan, J. R. Verbus, R. C. Webb, J. T. White, T. J. Whitis, M. S. Witherell, F. L. H. Wolfs, J. Xu, K. Yazdani, S. K. Young, and C. Zhang. First searches for axions and axionlike particles with the lux experiment. *Phys. Rev. Lett.*, 118:261301, Jun 2017.
- [41] Dmitry Budker, Peter W. Graham, Micah Ledbetter, Surjeet Rajendran, and Alexander O. Sushkov. Proposal for a cosmic axion spin precession experiment (casper). *Phys. Rev. X*, 4:021030, May 2014.
- [42] Asimina Arvanitaki and Andrew A. Geraci. Resonantly detecting axion-mediated forces with nuclear magnetic resonance. *Phys. Rev. Lett.*, 113:161801, Oct 2014.

- [43] Alexandre Payez, Carmelo Evoli, Tobias Fischer, Maurizio Giannotti, Alessandro Mirizzi, and Andreas Ringwald. Revisiting the SN1987a gamma-ray limit on ultralight axion-like particles. *Journal of Cosmology and Astroparticle Physics*, 2015(02):006–006, feb 2015.
- [44] Eder Izaguirre, Tongyan Lin, and Brian Shuve. Searching for Axionlike Particles in Flavor-Changing Neutral Current Processes. *Phys. Rev. Lett.*, 118(11):111802, 2017, [arXiv: 1611.09355 \[hep-ph\]](#).
- [45] Martin Bauer, Matthias Neubert, Sophie Renner, Marvin Schnubel, and Andrea Thamm. Flavor probes of axion-like particles. 10 2021, [arXiv: 2110.10698 \[hep-ph\]](#).
- [46] Kiwoon Choi, Hyungjin Kim, and Seokhoon Yun. Natural inflation with multiple sub-Planckian axions. *Phys. Rev. D*, 90:023545, 2014, [arXiv: 1404.6209 \[hep-th\]](#).
- [47] David E. Kaplan and Riccardo Rattazzi. Large field excursions and approximate discrete symmetries from a clockwork axion. *Phys. Rev. D*, 93(8):085007, 2016, [arXiv: 1511.01827 \[hep-ph\]](#).
- [48] Gian F. Giudice and Matthew McCullough. A Clockwork Theory. *JHEP*, 02:036, 2017, [arXiv: 1610.07962 \[hep-ph\]](#).
- [49] Marco Farina, Duccio Pappadopulo, Fabrizio Rompineve, and Andrea Tesi. The photo-philic QCD axion. *JHEP*, 01:095, 2017, [arXiv: 1611.09855 \[hep-ph\]](#).
- [50] N. Carrasco, P. Lami, V. Lubicz, L. Riggio, S. Simula, and C. Tarantino. $K \rightarrow \pi$ semileptonic form factors with $N_f = 2 + 1 + 1$ twisted mass fermions. *Phys. Rev. D*, 93(11):114512, 2016, [arXiv: 1602.04113 \[hep-lat\]](#).
- [51] G.Peter Lepage and Stanley J. Brodsky. Exclusive Processes in Perturbative Quantum Chromodynamics. *Phys. Rev. D*, 22:2157, 1980.
- [52] Stanley J. Brodsky and G. Peter Lepage. Large Angle Two Photon Exclusive Channels in Quantum Chromodynamics. *Phys. Rev. D*, 24:1808, 1981.
- [53] Adam Szczepaniak, Ernest M. Henley, and Stanley J. Brodsky. Perturbative {QCD} Effects in Heavy Meson Decays. *Phys. Lett. B*, 243:287–292, 1990.
- [54] Eduardo Cortina Gil et al. Search for π^0 decays to invisible particles. *JHEP*, 02:201, 2021, [arXiv: 2010.07644 \[hep-ex\]](#).

- [55] Eduardo Cortina Gil et al. Search for a feebly interacting particle X in the decay $K^+ \rightarrow \pi^+ X$. *JHEP*, 03:058, 2021, [arXiv: 2011.11329 \[hep-ex\]](#).
- [56] Eduardo Cortina Gil et al. Measurement of the very rare $K^+ \rightarrow \pi^+ \nu \bar{\nu}$ decay. [arXiv 2103.15389](#), [arXiv: 2103.15389 \[hep-ex\]](#).
- [57] Eduardo Cortina Gil et al. Search for K^+ decays to a muon and invisible particles. *Phys. Lett. B*, 816:136259, 2021, [arXiv: 2101.12304 \[hep-ex\]](#).
- [58] J.K. Ahn et al. Search for the $K_L \rightarrow \pi^0 \nu \bar{\nu}$ and $K_L \rightarrow \pi^0 X^0$ decays at the J-PARC KOTO experiment. *Phys. Rev. Lett.*, 122(2):021802, 2019, [arXiv: 1810.09655 \[hep-ex\]](#).
- [59] Eduard Masso and Ramon Toldra. On a light spinless particle coupled to photons. *Phys. Rev. D*, 52:1755–1763, 1995, [arXiv: hep-ph/9503293](#).
- [60] A.J. Bevan et al. The Physics of the B Factories. *Eur. Phys. J. C*, 74:3026, 2014, [arXiv: 1406.6311 \[hep-ex\]](#).
- [61] Matthew J. Dolan, Torben Ferber, Christopher Hearty, Felix Kahlhoefer, and Kai Schmidt-Hoberg. Revised constraints and Belle II sensitivity for visible and invisible axion-like particles. *JHEP*, 12:094, 2017, [arXiv: 1709.00009 \[hep-ph\]](#).
- [62] J. Grygier et al. Search for $B \rightarrow h \nu \bar{\nu}$ decays with semileptonic tagging at Belle. *Phys. Rev. D*, 96(9):091101, 2017, [arXiv: 1702.03224 \[hep-ex\]](#). [Addendum: *Phys.Rev.D* 97, 099902 (2018)].
- [63] W. Altmannshofer et al. The Belle II Physics Book. *PTEP*, 2019(12):123C01, 2019, [arXiv: 1808.10567 \[hep-ex\]](#). [Erratum: *PTEP* 2020, 029201 (2020)].
- [64] Xabier Cid Vidal, Alberto Mariotti, Diego Redigolo, Filippo Sala, and Kohsaku Tobioka. New Axion Searches at Flavor Factories. *JHEP*, 01:113, 2019, [arXiv: 1810.09452 \[hep-ph\]](#). [Erratum: *JHEP* 06, 141 (2020)].
- [65] Patrick deNiverville, Hye-Sung Lee, and Min-Seok Seo. Implications of the dark axion portal for the muon g-2, B-factories, fixed target neutrino experiments and beam dumps. *Phys. Rev. D*, 98(11):115011, 2018, [arXiv: 1806.00757 \[hep-ph\]](#).
- [66] Filippo Dattola. Search for $B^+ \rightarrow K^+ \nu \bar{\nu}$ decays with an inclusive tagging method at the Belle II experiment. In *55th Rencontres de Moriond on Electroweak Interactions and Unified Theories*, 5 2021, [arXiv: 2105.05754 \[hep-ex\]](#).

- [67] Roel Aaij et al. Search for hidden-sector bosons in $B^0 \rightarrow K^{*0} \mu^+ \mu^-$ decays. *Phys. Rev. Lett.*, 115(16):161802, 2015, [arXiv: 1508.04094 \[hep-ex\]](#).
- [68] R. Aaij et al. Search for long-lived scalar particles in $B^+ \rightarrow K^+ \chi(\mu^+ \mu^-)$ decays. *Phys. Rev. D*, 95(7):071101, 2017, [arXiv: 1612.07818 \[hep-ex\]](#).
- [69] P. A. Zyla et al. Review of Particle Physics. *PTEP*, 2020(8):083C01, 2020.
- [70] Bernard Aubert et al. A Search for Invisible Decays of the Upsilon(1S). *Phys. Rev. Lett.*, 103:251801, 2009, [arXiv: 0908.2840 \[hep-ex\]](#).
- [71] A.V. Efremov and A.V. Radyushkin. Factorization and asymptotic behaviour of pion form factor in qcd. *Physics Letters B*, 94(2):245–250, 1980.
- [72] George F. Sterman and Paul Stoler. Hadronic form-factors and perturbative QCD. *Ann. Rev. Nucl. Part. Sci.*, 47:193–233, 1997, [arXiv: hep-ph/9708370](#).
- [73] Sidney D. Drell and Tung-Mow Yan. Connection of elastic electromagnetic nucleon form factors at large Q^2 and deep inelastic structure functions near threshold. *Phys. Rev. Lett.*, 24:181–186, Jan 1970.
- [74] A. Duncan and Alfred H. Mueller. Asymptotic Behavior of Exclusive and Almost Exclusive Processes. *Phys. Lett. B*, 90:159–163, 1980.
- [75] Vladimir M. Braun. Light cone sum rules. In *4th International Workshop on Progress in Heavy Quark Physics*, pages 105–118, 9 1997, [arXiv: hep-ph/9801222](#).
- [76] Xing-Gang Wu and Tao Huang. Heavy and light meson wavefunctions. *Chin. Sci. Bull.*, 59:3801, 2014, [arXiv: 1312.1455 \[hep-ph\]](#).
- [77] A. V. Radyushkin. Deep Elastic Processes of Composite Particles in Field Theory and Asymptotic Freedom. 6 1977, [arXiv: hep-ph/0410276](#).
- [78] Tao Huang, Tao Zhong, and Xing-Gang Wu. Determination of the pion distribution amplitude. *Phys. Rev. D*, 88:034013, 2013, [arXiv: 1305.7391 \[hep-ph\]](#).
- [79] V. L. Chernyak and A. R. Zhitnitsky. Exclusive Decays of Heavy Mesons. *Nucl. Phys. B*, 201:492, 1982. [Erratum: *Nucl.Phys.B* 214, 547 (1983)].
- [80] A. Erdélyi, W. Magnus, F. Oberhettinger, and F.G. Tricomi. *Higher Transcendental Functions. Vol. II*. McGraw-Hill, 1953.

- [81] G. Peter Lepage and Stanley J. Brodsky. Exclusive processes in quantum chromodynamics: Evolution equations for hadronic wavefunctions and the form factors of mesons. *Physics Letters B*, 87(4):359–365, 1979.
- [82] A. V. Efremov and A. V. Radyushkin. Factorization and Asymptotical Behavior of Pion Form-Factor in QCD. *Phys. Lett. B*, 94:245–250, 1980.
- [83] S. V. Mikhailov and A. V. Radyushkin. The Pion wave function and QCD sum rules with nonlocal condensates. *Phys. Rev. D*, 45:1754–1759, 1992.
- [84] A.H. Mueller. Perturbative qcd at high energies. *Physics Reports*, 73(4):237–368, 1981.
- [85] Bhubanjoyoti Bhattacharya, Cody M. Grant, and Alexey A. Petrov. Invisible widths of heavy mesons. *Phys. Rev. D*, 99(9):093010, 2019, [arXiv: 1809.04606 \[hep-ph\]](#).
- [86] Derek E. Hazard and Alexey A. Petrov. Lepton flavor violating quarkonium decays. *Phys. Rev. D*, 94(7):074023, 2016, [arXiv: 1607.00815 \[hep-ph\]](#).
- [87] Martin Bauer, Matthias Neubert, and Andrea Thamm. Collider Probes of Axion-Like Particles. *JHEP*, 12:044, 2017, [arXiv: 1708.00443 \[hep-ph\]](#).
- [88] Nico Gubernari, Ahmet Kokulu, and Danny van Dyk. $B \rightarrow P$ and $B \rightarrow V$ Form Factors from B -Meson Light-Cone Sum Rules beyond Leading Twist. *JHEP*, 01:150, 2019, [arXiv: 1811.00983 \[hep-ph\]](#).
- [89] Patricia Ball. The Semileptonic decays $D \rightarrow \pi(\rho) e \nu$ and $B \rightarrow \pi(\rho) e \nu$ from QCD sum rules. *Phys. Rev. D*, 48:3190–3203, 1993, [arXiv: hep-ph/9305267](#).
- [90] Patricia Ball and Roman Zwicky. $B_{d,s} \rightarrow \rho, \omega, K^*, \phi$ decay form-factors from light-cone sum rules revisited. *Phys. Rev. D*, 71:014029, 2005, [arXiv: hep-ph/0412079](#).
- [91] Patricia Ball and Roman Zwicky. New results on $B \rightarrow \pi, K, \eta$ decay form-factors from light-cone sum rules. *Phys. Rev. D*, 71:014015, 2005, [arXiv: hep-ph/0406232](#).
- [92] Wei Wang and Yue-Long Shen. $D_s \rightarrow K, K^*, \phi$ form factors in the Covariant Light-Front Approach and Exclusive D_s Decays. *Phys. Rev. D*, 78:054002, 2008.

- [93] Wei Wang, Yue-Long Shen, and Cai-Dian Lu. Covariant Light-Front Approach for B(c) transition form factors. *Phys. Rev. D*, 79:054012, 2009, [arXiv: 0811.3748 \[hep-ph\]](#).
- [94] Aidos Issadykov, Mikhail A. Ivanov, and Sayabek K. Sakhiyev. Form factors of the B-S-transitions in the covariant quark model. *Phys. Rev. D*, 91(7):074007, 2015, [arXiv: 1502.05280 \[hep-ph\]](#).
- [95] V. Lubicz, L. Riggio, G. Salerno, S. Simula, and C. Tarantino. Scalar and vector form factors of $D \rightarrow \pi(K)\ell\nu$ decays with $N_f = 2 + 1 + 1$ twisted fermions. *Phys. Rev.*, D96(5):054514, 2017, [arXiv: 1706.03017 \[hep-lat\]](#). [erratum: *Phys. Rev.* D99,no.9,099902(2019); Erratum: *Phys. Rev.* D100,no.7,079901(2019)].
- [96] Yuzhi Liu et al. $B_s \rightarrow K\ell\nu$ Form Factors with 2+1 Flavors. *EPJ Web Conf.*, 175:13008, 2018, [arXiv: 1711.08085 \[hep-lat\]](#).
- [97] Laurence J. Cooper, Christine T.H. Davies, Judd Harrison, Javad Komijani, and Matthew Wingate. $B_c \rightarrow B_{s(d)}$ form factors from lattice QCD. *Phys. Rev. D*, 102(1):014513, 2020, [arXiv: 2003.00914 \[hep-lat\]](#).
- [98] Hai-Bing Fu, Xing-Gang Wu, Hua-Yong Han, and Yang Ma. B $\rightarrow \rho$ transition form factors and the ρ -meson transverse leading-twist distribution amplitude. *J. Phys. G*, 42(5):055002, 2015, [arXiv: 1406.3892 \[hep-ph\]](#).
- [99] Aoife Bharucha, David M. Straub, and Roman Zwicky. $B \rightarrow V\ell^+\ell^-$ in the Standard Model from light-cone sum rules. *JHEP*, 08:098, 2016, [arXiv: 1503.05534 \[hep-ph\]](#).
- [100] E. McLean, C. T. H. Davies, A. T. Lytle, and J. Koponen. Lattice QCD form factor for $B_s \rightarrow D_s^*\ell\nu$ at zero recoil with non-perturbative current renormalisation. *Phys. Rev. D*, 99(11):114512, 2019, [arXiv: 1904.02046 \[hep-lat\]](#).
- [101] E. McLean, C. T. H. Davies, A. T. Lytle, and J. Koponen. $B_s \rightarrow D_s^{(*)}\ell\nu$ form factors using heavy HISQ quarks. *PoS*, LATTICE2018:281, 2019, [arXiv: 1901.04979 \[hep-lat\]](#).
- [102] Matthew J. Dolan, Felix Kahlhoefer, Christopher McCabe, and Kai Schmidt-Hoberg. A taste of dark matter: Flavour constraints on pseudoscalar mediators. *JHEP*, 03:171, 2015, [arXiv: 1412.5174 \[hep-ph\]](#). [Erratum: *JHEP* 07, 103 (2015)].
- [103] N. Satoyama et al. A Search for the rare leptonic decays $B^+ \rightarrow \mu^+ \nu(\mu)$ and $B^+ \rightarrow e^+ \nu(\nu)$. *Phys. Lett. B*, 647:67–73, 2007, [arXiv: hep-ex/0611045](#).

- [104] M. T. Prim et al. Search for $B^+ \rightarrow \mu^+ \nu_\mu$ and $B^+ \rightarrow \mu^+ N$ with inclusive tagging. *Phys. Rev. D*, 101(3):032007, 2020, [arXiv: 1911.03186 \[hep-ex\]](#).
- [105] I. Adachi et al. Evidence for $B^- \rightarrow \tau^- \bar{\nu}_\tau$ with a Hadronic Tagging Method Using the Full Data Sample of Belle. *Phys. Rev. Lett.*, 110(13):131801, 2013, [arXiv: 1208.4678 \[hep-ex\]](#).
- [106] B.I. Eisenstein et al. Precision Measurement of $B(D^+ \rightarrow \mu^+ \nu)$ and the Pseudoscalar Decay Constant $f(D^+)$. *Phys. Rev. D*, 78:052003, 2008, [arXiv: 0806.2112 \[hep-ex\]](#).
- [107] M. Ablikim et al. Precision measurements of $B(D^+ \rightarrow \mu^+ \nu_\mu)$, the pseudoscalar decay constant f_{D^+} , and the quark mixing matrix element $|V_{cd}|$. *Phys. Rev. D*, 89(5):051104, 2014, [arXiv: 1312.0374 \[hep-ex\]](#).
- [108] Medina Ablikim et al. Determination of the pseudoscalar decay constant $f_{D_s^+}$ via $D_s^+ \rightarrow \mu^+ \nu_\mu$. *Phys. Rev. Lett.*, 122(7):071802, 2019, [arXiv: 1811.10890 \[hep-ex\]](#).
- [109] Medina Ablikim et al. Measurement of the $D_s^+ \rightarrow \ell^+ \nu_\ell$ branching fractions and the decay constant $f_{D_s^+}$. *Phys. Rev. D*, 94(7):072004, 2016, [arXiv: 1608.06732 \[hep-ex\]](#).
- [110] Medina Ablikim et al. Observation of the leptonic decay $D^+ \rightarrow \tau^+ \nu_\tau$. *Phys. Rev. Lett.*, 123(21):211802, 2019, [arXiv: 1908.08877 \[hep-ex\]](#).
- [111] A. Zupanc et al. Measurements of branching fractions of leptonic and hadronic D_s^+ meson decays and extraction of the D_s^+ meson decay constant. *JHEP*, 09:139, 2013, [arXiv: 1307.6240 \[hep-ex\]](#).
- [112] C. Lazzeroni et al. Precision Measurement of the Ratio of the Charged Kaon Leptonic Decay Rates. *Phys. Lett. B*, 719:326–336, 2013, [arXiv: 1212.4012 \[hep-ex\]](#).
- [113] F. Ambrosino et al. Measurement of the charged kaon lifetime with the KLOE detector. *JHEP*, 01:073, 2008, [arXiv: 0712.1112 \[hep-ex\]](#).